CLEARINGHOUSE FOR FEDERAL SCIENTIFIC AND TECHNICAL INFORMATION CFSTI
DOCUMENT MANAGEMENT BRANCH 410.11

LIMITATIONS IN REPRODUCTION QUALITY

ACCESSION #

☐ 1. WE REGRET THAT LEGIBILITY OF THIS DOCUMENT IS IN PART UNSATISFACTORY. REPRODUCTION HAS BEEN MADE FROM BEST AVAILABLE COPY.

☒ 2. A PORTION OF THE ORIGINAL DOCUMENT CONTAINS FINE DETAIL WHICH MAY MAKE READING OF PHOTOCOPY DIFFICULT.

☐ 3. THE ORIGINAL DOCUMENT CONTAINS COLOR, BUT DISTRIBUTION COPIES ARE AVAILABLE IN BLACK-AND-WHITE REPRODUCTION ONLY.

☐ 4. THE INITIAL DISTRIBUTION COPIES CONTAIN COLOR WHICH WILL BE SHOWN IN BLACK-AND-WHITE WHEN IT IS NECESSARY TO REPRINT.

☐ 5. LIMITED SUPPLY ON HAND: WHEN EXHAUSTED, DOCUMENT WILL BE AVAILABLE IN MICROFICHE ONLY.

☐ 6. LIMITED SUPPLY ON HAND: WHEN EXHAUSTED DOCUMENT WILL NOT BE AVAILABLE.

☐ 7. DOCUMENT IS AVAILABLE IN MICROFICHE ONLY.

☐ 8. DOCUMENT AVAILABLE ON LOAN FROM CFSTI (TT DOCUMENTS ONLY).

☐ 9.

NBS 9/64 PROCESSOR:

Copy No. 146

Document No. 56-6924
Copy No. 1

AMP Report 42. 2R
AMG-NYU No. 133

UNCLASSIFIED

THE FORCE OF IMPACT ON A SPHERE STRIKING A WATER SURFACE

SECOND APPROXIMATION

Prepared for the
APPLIED MATHEMATICS PANEL
NATIONAL DEFENSE RESEARCH COMMITTEE
By the
Applied Mathematics Group
New York University

UNCLASSIFIED

July 1945

56-6924 C-1

~~CONFIDENTIAL~~

REG NO. ____ Prepared under Contract OEMsr-945

LOG NO 12532

WDSIT 405-7

Approved for distribution
Warren Weaver
Chief, Applied Mathematics Panel

Distribution List
AMP Report 42.2R

Copy No.	
1 - 8	Office of the Executive Secretary, OSRD
9 - 51	Liaison Office, OSRD
52 - 53	Ordnance Research Center, Aberdeen Proving Ground 1 Att: T. L. Smith
54 - 56	Commanding General, Army Air Forces Att: T. von Karman
57 - 60	Chief, Bureau of Ordnance 1 R. S. Burington 1 Comdr. S. Brunauer 1 Lt. Comdr. W. E. Bleick
61 - 62	Office of the Chief of Ordnance 1 H. M. Morse 1 Capt. D. D. Johnston
63 - 65	Director, David Taylor Model Basin 1 W. H. Bowers 1 E. H. Kennard
66 - 67	Director, Naval Ordnance Laboratory 1 Capt. R. D. Bennett 1 Ens. D. Gilbarg
68	Director, Naval Research Laboratory Att: G. R. Irwin
69	Naval Torpedo Station, Newport Att: Lt. Comdr. H. C. Pavian
70 - 71	E. B. Wilson, Chief, Division 2 1 Woods Hole Oceanographic Institute
72 - 73	F. L. Hovde, Chief, Division 3 1 L. Slichter 1 S. Bowen
74 - 82	J. T. Tate, Chief, Division 6 1 C. Herring 1 M. Gimprich 1 F. C. Lindvall 2 R. T. Knapp 1 L. G. Straub 1 W. V. Houston

[redacted]

[redacted]

Copy No.

83 Commanding General, AAF Materiel Command, Wright Field
Att: Capt. J. F. Healy

84 Commanding General, AAF Proving Ground Command, Elgin Field
Att: Col. R. T. Huff

85 W. Weaver, Chief, Applied Mathematics Panel

86 T. C. Fry, Acting Chief, Applied Mathematics Panel

87 L. M. Graves

88 O. Veblen

89 - 92 R. Courant
1 M. Shiffman
1 D. C. Spencer

93 S. S. Wilks

94 I. S. Sokolnikoff

95 M. Rees

96 - 98 Garrett Birkhoff
1 Norman Levinson
1 Lynn Loomis

99 J. G. Kirkwood

100 F. D. Murnaghan

101 Committee on Medical Research
Att: E. Newton Harvey

[redacted]

Table of Contents

[redacted]

PREFACE

In a previous report (AMP Report 42.1R), the problem of vertical impact of a body with a spherical nose on a water-surface was solved mathematically by Max Shiffman and Donald C. Spencer of the New York University Group of the Applied Mathematics Panel. The solution was based on the assumption that the surface of the water is not appreciably altered by the entry of the body, an assumption which can be accepted only as a first approximation.

Therefore, a further study was undertaken, taking into account the disturbance of the surface of the water. The present report presents the results of these studies. It is shown that the disturbance of the surface leads to two types of corrections of the previous results. In the first place, the upward rise of the surface of the water wets a larger portion of the entering body, thereby increasing the resistance of the water to the entering body. Secondly, the rising surface relaxes somewhat the restraint imposed on the body, causing a decrease in the impact force. These two corrections, which partly counterbalance one another, are analyzed here by using a combination of theory and information derived from experiment. The final result, which deviates somewhat from the first approximation, is compared with experiment and shown to be in satisfactory agreement with it.

With the experience gained and the theory developed for vertical entry, it is hoped that the impact forces during oblique entry will be amenable to treatment. This question is now being considered by the same authors.

Attention should be drawn to the work of the Harvard Group of the Applied Mathematics Panel concerning air-water entry as a whole, and to the activities of the Underwater Ballistics Committee.

The writers were greatly helped by other members of the New York University Group, in particular by Mr. M. H. Shamos, who made an important contribution by excellent flash photographs he took of spheres entering water. These photographs furnished much qualitative and numerical information. Thanks are also due to Dr. Patrick Hurley of the Morris Dam Group of the California Institute of Technology for permission to use the photographs exhibited in Plate 5; to Dr. R. M. Davies of the Engineering Laboratory, Cambridge, England for Plate 6; and to Dr. E. Newton Harvey of Princeton University for Plate 7.

R. Courant

Director, Contract OEMsr-945

[redacted]

THE FORCE OF IMPACT ON A SPHERE STRIKING A WATER SURFACE

Second Approximation

Section 1. Introduction and Summary

The entry of a solid body from air into water may take place in two ways: (i) if the speed is small and if the surface of the body is smooth, the entry occurs without the formation of a cavity (smooth entry); (ii) if the speed is great or if the surface of the body is rough or has an irregular shape, the flow detaches from the body when it has penetrated a short distance below the initial surface level (rough entry). In either case there is an initial period following contact with the surface during which the body experiences the greatest deceleration and which is of such short duration that cavitation has not yet developed. The determination of the forces acting during this impact stage of the entry is important in the case of projectiles shot or dropped into water, not only because of possible damage to the mechanism and nose but also because the impulsive forces and torques created by the impact influence the underwater trajectory of the projectile.

We suppose that the nose of the projectile is spherical in shape and that the initial impact with the surface is vertical. We may then visualize the mass of the projectile as concentrated into a sphere of the same radius as the nose. In a previous report [25]* we obtained a first approximation to the force of impact on a sphere entering vertically by disregarding the rise of the surface; in the present report we obtain a second approximation by estimating the effects of the surface motion and we compare our theoretical estimates with experiment.

---

* Numbers in brackets [ ] refer to the bibliography at the end of this report.

The resultant upward force P acting on the sphere in the impact stage can be expressed in terms of a dimensionless impact-drag coefficient C_p. Let A be the radius of the sphere, U_o its initial velocity upon impact, and ρ the density of water. Then the impact force may be conveniently expressed as

$$P = \frac{1}{2}\rho U_o^2 \cdot \pi A^2 \cdot C_p$$

where C_p is the "impact-drag coefficient." The coefficient C_p depends on the time; it is zero when the sphere first strikes the surface, rapidly increases to a maximum value, and then decreases.

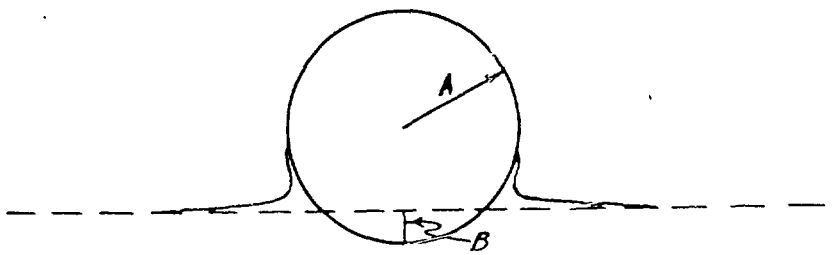

The impact-drag coefficient C_p may be expressed in terms of the "virtual mass" of the fluid. If U is the velocity of the sphere at time t, we define the virtual mass of the fluid to be a quantity M such that MU is the total vertical impulse communicated to the fluid during the time interval t; in other words M is defined by the equation

$$P = \frac{d}{dt}(MU) .$$

Let B denote the depth of penetration of the bottom of the sphere below the initial surface level, and let $b = B/A$.

Introducing the additional dimensionless quantity $m = M/\frac{1}{2}\pi\rho A^3$, we obtain in Section 3 the formula

$$C_p = \frac{\frac{dm}{db}}{(1 + \frac{3m}{8\sigma})^3}$$

where σ is the "specific gravity" of the incoming projectile considered as though the whole mass were concentrated into a sphere having the same radius as the nose,

$$\sigma = \frac{\text{mass of projectile}}{\frac{4}{3}\pi\rho A^3} .$$

Our final estimate of C_p as a function of b is plotted in Graph 1 for various valuos of σ. (All graphs are collected together at the end of the report. For the sake of convenience, Graph 1 is also inserted on the next page.) For values of σ ranging from 1 to ∞, the impact drag coefficient C_p rises very rapidly to a peak of about 1, the peak occurring when the sphere has penetrated to a distance of from 0.1 to 0.2 of a radius below the initial surface level. The coefficient C_p then declines more slowly, until at about 0.7 of a radius of entry its value is equal to the stationary cavity drag value of 0.3 (for description of cavity drag, see [2] and [21]).

For smaller values of σ, this general behavior of C_p is retained but is shifted downward and to the left.

The question arises whether, in rough entry, the cavity formation which takes place will interfere with the above results and partly vitiate them. It is known from both experimental and theoretical grounds that the cavity begins to form only after the sphere has submerged a distance somewhere between a quarter of a radius and a radius. Thus the behavior of C_p depicted in Graph 1 still applies --- the rapid rise of C_p to a

Graph 1 Impact Drag Coefficient

$$C_p = \frac{\frac{dm}{db}}{\left(1 + \frac{3m}{8\sigma}\right)^3}$$

where σ = mass of incoming projectile / $\frac{4}{3}\pi\rho A^3$

C_p

1.00
.80
.60
.40
.20
0

$\sigma = 8$
$\sigma = 1.0$
$\sigma = 0.5$
$\sigma = 0.25$

.1 .2 .3 .4 .5 .6 .7 .8 .9 1.0

$b \rightarrow$

maximum of about 1, and the slower decline to the cavity drag value of 0.3. The brief impact stage in rough entry is the same as in smooth entry.

The dimensionless virtual mass m defined by $m = M/\frac{1}{2}\pi\rho A^3$ is plotted as a function of b in Graph 3. For purposes of comparison we have plotted in the same graph our first approximation for m, taken from the previous report [15]. Likewise, in Graph 2, our corrected estimate of C_p in the case $\sigma = \infty$ is compared with our first approximation obtained in [15]. In the corrected estimate, the maximum of C_p is somewhat larger and is displaced to the left.

The first approximation of the impact-drag coefficient was derived in our report [15] under the assumption that the surface does not rise, the surface remaining plane and at its initial level. Under these circumstances the flow at each instant t depends only on the depth of penetration below the initial level and on the velocity of the sphere at that instant t and is otherwise independent of the past history of the entry; for this reason the flow might be called "quasi-steady."

In the present report a second approximation is obtained which takes into account the past history of the phenomenon. The corrections are of two sorts. On the one hand the water rises and wets a larger portion of the spherical surface than it would if the surface did not rise. The fluid therefore exerts pressure over a larger area and increases the total impact force. This will be called the "wetting correction." On the other hand, the free surface rises and relaxes to a certain extent the restraint imposed on the sphere. This will be called the "surface correction." These two corrections are discussed in Sections 6 and 7 respectively, and both are combined in Section 8 to give the final estimate of the impact-drag coefficient C_p.

In Section 9 this final estimate of C_p is compared with experimental measurements of the impact force on a sphere.

Comparison is made with measurements taken by S. Watanabe's [17] in 1930, who used a piezoelectric gauge to determine the force; with rough experiments of R. W. Blundell [3] made in 1937; and with recent measurements of E. G. Richardson [13].

Watanabe's experiments were very carefully performed with accurate instruments and verified the fact that the impact force varies as the square of the initial velocity. The value of the specific gravity σ of the sphere in Watanabe's experiment was as low as 0.116. The theoretical C_p curve corresponding to this value of σ is compared with Watanabe's experimental curve in Graph 10. Note that the range of b is small, from 0 to .03. The agreement is remarkably good for very small values of b, when C_p is increasing rapidly. In fact, near $b = 0$ the theory gives

$$C_p = 6.62\, b^{1/2} - a_2 b + \cdots$$

where the constant a_2 is not accurately determined by the theory. The first term $6.62 b^{1/2}$ of this expansion is verified completely by Watanabe's data. The deviation in the remaining portion of the curve is due to the second coefficient a_2.

In Blundell's experiment, σ ranged from .2 and .3 approximately. The experimental curves, transcribed to the dimensionless form of a drag coefficient, are shown in Graph 11(a), and the corresponding theoretical curves are drawn in Graph 11(b). An idea of the rather large experimental error may be seen by comparing curves (B) and (C) which should be identical, and from the fact that curve (D) should be the highest (since σ is the largest). The experiments at least give an idea of the order of magnitude of the impact forces and of their duration, and the agreement with theory is satisfactory. In fact, curve (D) even agrees numerically with theory.

In Richardson's experiment, $\sigma = .16$. The corresponding theoretical curve is compared with Richardson's in Graph 12,

and the agreement is fair. Again, Richardson's experiment should be considered as yielding only the order of magnitude of C_p.

In each of these experiments, the value of σ is small. It would be desirable to carry out experiments with larger values of σ, using accurate instruments (such as piezoelectric gauges).

In addition to the impact force, it is of interest to know the average pressure $\bar{p}$ acting over the portion of the sphere in contact with the water. This pressure can be written in the form

$$\bar{p} = \frac{1}{2}\rho U_o^2 \cdot D_p$$

where D_p is a dimensionless coefficient. The dependence of D_p on $b = B/A$ is shown in Graph 4 (for the case $\sigma = \infty$). It is noteworthy that the value of D_p at the initial contact of the sphere with the water is infinite. Actually, because of the compressibility of the water and because of the fact that the compression wave is initially a plane wave, the pressure $\bar{p}$ during this phase is approximately cU_o where c is the speed of sound in water. This would give a value of D_p approximately equal to $\frac{2c}{U_o}$. The intersection of the straight line $D_p = \frac{2c}{U_o}$ with Graph 4 gives an indication of the time interval in which compressibility plays a role.* Thus, the effect of compressibility

---

* Using the asymptotic formula

$$D_p = \frac{2.2}{6^{1/2}}$$

for small b, and equating this to $\frac{2c}{U_o}$, one obtains

$$b = \left(\frac{U_o}{c}\right)^2$$

as an estimate of the relative depth of penetration in which compressibility plays a role. Even if the initial entry velocity U_o is as high as 500 ft/sec this yields $b = .01$, an order of magnitude which is negligible.
This idea was also suggested by M. Gimprich.

is to reduce the value of D_p and therefore of C_p at the very beginning.

Concerning the actual distribution of pressure over the wetted portion of the sphere, we remark that the pressure is not greatest at the lowest point of the sphere (stagnation point). This fact arises from the non-stationary character of the flow, and the usual conceptions based on stationary flow do not apply. On the contrary, the pressure is a minimum at the lowest point of the sphere and has a very sharp and high maximum near the edge of the wetted portion of the sphere. This fact was derived theoretically by Wagner [16] in the two-dimensional case of the entry of a very flat wedge. However, an estimate of the depth at which stationary flow approximately sets in can be obtained by determining when C_p is about 0.3. This occurs for $b = .7$ approximately.

Section 2. Photographs of Entry

The interesting sequence of events produced by entry of a sphere from air into water was first photographed and described by Worthington [19]. Plate 1 is a reproduction of some of his photographs and shows several stages in the smooth entry of a sphere. A more complete sequence, which shows the splash in greater detail, is given in Plates 2,3. As may be observed from these two sets of pictures the phenomena accompanying smooth entry are closely duplicated in different experiments. Even the jets produced as the water envelopes the spheres differ little in appearance.

In order to show more clearly the splash during impact, an enlarged photograph is reproduced in Plate 4. We observe that the splash is largely concentrated in the immediate neighborhood of the sphere and is composed of a relatively thick base from which a thin sheath rises up along the sides of the sphere. A few drops which have detached themselves may be seen at the top of the sheath.

Because of the speed with which projectiles are usually launched into water their entry is rough. In fact, the entry of a bomb, mine, or torpedo takes place in three stages: (i) the initial impact stage which begins when the projectile touches the surface and ends when cavitation developes; (ii) motion through the water with a trailing cavity extending to the surface; (iii) motion after the cavity is closed. The closure of the cavity takes place either at the surface or below the surface, but in either case the projectile carries with it a pulsating air bubble which gradually disappears.

The initial stage of the rough entry of a sphere is shown in Plate 5. The sheath, which persists alongside the sphere in the case of smooth entry, detaches in rough entry and may break up into spray. However, the thick base of the splash remains in contact with the sphere and is the same as in smooth entry. So far as estimation of impact force is concerned, the effect of the sheath is negligible compared to that of the thick base.

The further stages of rough entry are shown in Plate 6. Unfortunately only the first photograph shows the sphere in the impact phase and here the splash cannot be seen very clearly. However, the sheath can be seen as a light band surrounding the sphere above the surface.

For the usual projectile entering water the speed does not exceed five or ten percent of sound speed in water. It is therefore reasonable to neglect compressibility effects. For the sake of general interest, we include Plate 7, which shows a sphere entering at roughly half the speed of sound in water. Here the effect of the compressibility is of course important.

Section 3. Virtual Mass

The impact drag coefficient C_p will be obtained in terms of the "virtual mass" M of the fluid. Let U be the downward

velocity of the sphere at any instant t, and let P be the resultant upward impact force exerted on the sphere. Then the sphere exerts a downward force P on the fluid and imparts momentum to the fluid. The "virtual mass" M of the fluid at a given instant t is defined by*

$$(3.1) \qquad P = \frac{d}{dt}(MU) \quad \text{or} \quad MU = \int_0^t P\,dt \ .$$

Let M_0 be the mass of the incoming projectile. Neglecting gravity compared to the impact force P, we have

$$(3.2) \qquad -P = \frac{d}{dt}(M_0 U) \ .$$

Adding (3.1) and (3.2) we obtain $\frac{d}{dt}\left[(M + M_0)\,U\right] = 0$ and so integrating,

$$(3.3) \qquad (M + M_0)U = M_0 U_0 \quad \text{or} \quad U = \frac{U_0}{1 + M/M_0}$$

where U_0 is the velocity of the incoming sphere at the initial instant of contact with the fluid.

Let $B = B(t)$ be the distance at time t of the lowest point of the sphere from the initial surface level; the velocity U of the sphere is then $\dot{B} = \frac{dB}{dt}$. By differentiating (3.3) with

---

* Thus MU is the vertical impulse contributed to the fluid by the moving sphere. It is also possible to introduce a virtual mass based on the kinetic energy of the fluid, but for the case of impact it differs from the virtual mass defined above. This is to be expected from general considerations of inelastic impact. We shall use throughout this report the definition (3.1) of the virtual mass, based on momentum; justification of this choice is given in the Appendix.

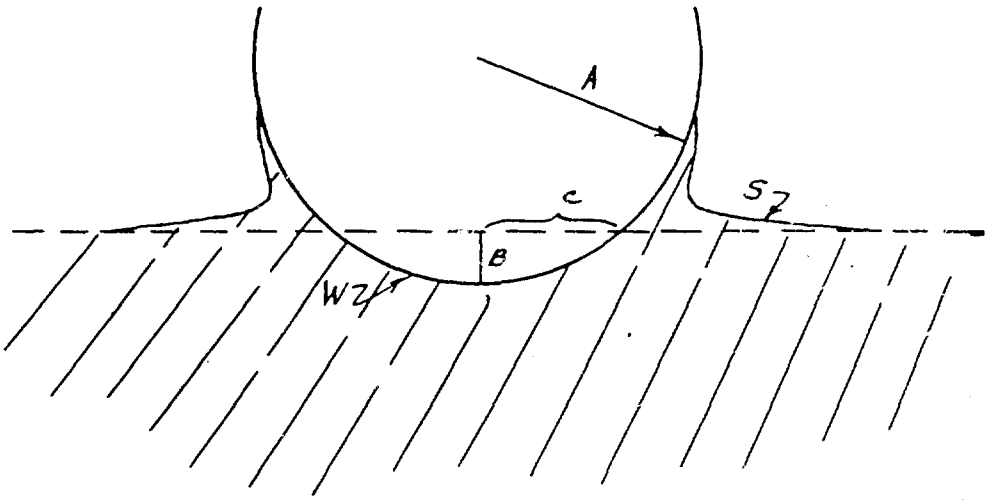

respect to t and using (3.2), it follows that

$$P = \frac{dM/dB}{1 + \frac{M}{M_o}} U^2 = \frac{dM/dB}{(1 + \frac{M}{M_o})^3} U_o^2 \quad . \tag{3.4}$$

Let A denote the radius of the incoming sphere, and let ρ be the density of water. Introducing the dimensionless quantities

$$m = \frac{M}{\frac{1}{2}\pi\rho A^3} \quad , \; b = \frac{B}{A} \; , \tag{3.5}$$

we may write

$$P = \frac{1}{2}\rho U_o^2 \cdot \pi A^2 \cdot C_p \tag{3.6}$$

where

$$C_p = \frac{\frac{dm}{db}}{(1 + \frac{M}{M_o})^3} \quad . \tag{3.7}$$

For incoming projectiles of large mass compared to the mass of the water displaced by the hemispherical nose, $\frac{M}{M_o}$ may be neglected compared to 1. Then the impact drag coefficient C_p is merely $\frac{dm}{db}$. Also, from (3.3), the change in velocity U in the impact stage is small.

However, if M_o is not large compared to M, the denominator in (3.2) must be retained. This is the case in the experiments which will be cited in Section 9, and it is convenient to put the denominator in a slightly different form. Let σ be the specific gravity of the incoming projectile considered as though the whole mass were concentrated into a sphere (if the incoming projectile is not already a sphere), i.e.,

$$\sigma = \frac{M_o}{\frac{4}{3}\pi\rho A^3} \quad . \tag{3.8}$$

Using (3.5), equation (3.7) may be written

$$C_p = \frac{\frac{dm}{db}}{(1 + \frac{3}{8\sigma} m)^3} \quad . \tag{3.9}$$

The determination of the impact-drag coefficient C_p requires merely the determination of the dimensionless virtual mass m.

Section 4. Hydrodynamic Formulation of the Problem.

We shall neglect the effects of compressibility and of the viscosity of the fluid. Since the fluid is at rest before the sphere strikes it, the flow of the fluid at each instant of time t is irrotational and can be described by a velocity potential ψ. This is a function $\psi(x, y, z, t)$ defined over the region of space occupied by the fluid such that

$$-\operatorname{grad} \psi$$

is the velocity of the fluid at the instant t and the position

x, y, z. The velocity potential, on account of the incompressibility of the fluid, satisfies the potential equation

$$\psi_{xx} + \psi_{yy} + \psi_{zz} = 0 ,$$

where subscripts mean differentiation. The potential is normalized by setting $\psi = 0$ at ∞). The pressure in the fluid is connected with the potential function by the Bernoulli equation

$$\frac{p}{\rho} + \frac{1}{2} (\text{grad}\,\psi)^2 - \frac{\partial \psi}{\partial t} = 0 \tag{4.1}$$

where p is the pressure in excess of hydrostatic pressure.

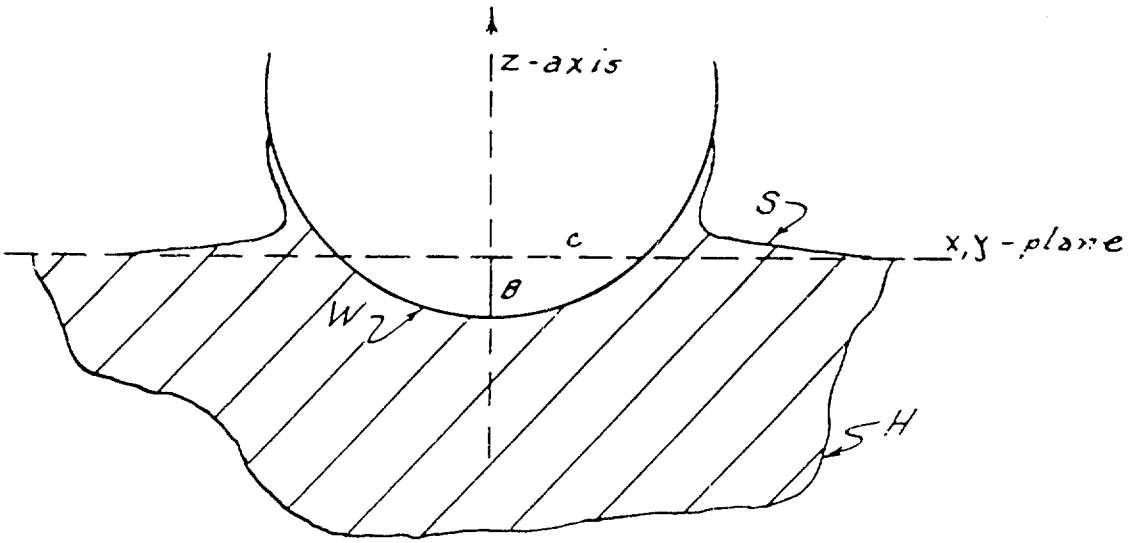

To obtain the impact force exerted on the sphere, we shall use the principle of conservation of momentum. The total momentum of the fluid is directed vertically downward because of the rotational symmetry and is equal to

$$(4.2) \qquad \iiint \rho \frac{\partial \psi}{\partial z}\, dxdydz = \rho \iint_{W+S} \psi\, dxdy - \rho \iint_{H_\infty} \psi\, dxdy \ .$$

Here W is the wetted portion of the sphere, S is the free surface, and the last term in (4.2) means the limit of the integral $\iint \psi\, dxdy$ extended over the submerged portion H of a large spherical surface the radius of which tends to infinity.

The external forces acting on the fluid contained in the membrane H are: (i) the downward force of magnitude P exerted by the sphere and (ii) the upward force exerted on H by the pressure of the fluid external to it. (The resultant force due to the constant atmospheric pressure is zero. The only effect of gravity is the buoyancy which is negligible compared to the impact force P.) The force (ii) is equal to the time rate of change of the last term in (4.2). For, by Bernoulli's law (4.1), the force (ii) differs from the time rate of change of the last term by a term of the form

$$\iint_H (\operatorname{grad} \psi)^2\, dxdy$$

which approaches zero as the radius of H becomes infinite. (For, at ∞, ψ behaves at worst like $\frac{1}{R}$, therefore $(\operatorname{grad} \psi)^2$ like $\frac{1}{R^4}$ and the whole integral like $\frac{1}{R^2}$). Likewise the momentum flux through the surface H consists of integrals of squares of velocities, and these approach zero as the radius of H becomes infinite. Since the resultant of all the external forces is equal to the time rate of change of the momentum (4.2), we therefore have

$$(4.3) \qquad P = \frac{d}{dt} \left(\rho \iint \psi\, dxdy \right) \ .$$

The formula (4.3) can also be inferred directly from the known physical interpretation of the potential function ψ, namely that $\rho\psi$ is the impulsive pressure required to produce the flow.

It is convenient to exhibit separately the effect of the velocity $\dot{B}$ of the sphere by setting

$$\psi(x, y, z, t) = \dot{B}\phi(x, y, z, t) , \tag{4.4}$$

so that ϕ is the instantaneous potential function corresponding to the parameter B and to unity as velocity of the sphere. Then (4.3) can be written

$$P = \frac{d}{dt} (M\dot{B})$$

where

$$M = \rho \iint_{W+S} \phi \, dx dy \quad . \tag{4.5}$$

This formula expresses the virtual mass of the fluid in terms of the potential function ϕ.

Section 5. The First Approximation for a Sphere

Consider the flow produced in the fluid as a result of the entry of the sphere. As the sphere penetrates the surface, the free surface no longer remains plane but rises slightly and forms spurts running up the sides of the sphere. Although the exact shape of the surface is difficult to determine theoretically, some estimates will be presented in Section 6. For the purpose of computing the virtual mass and the impact force, we shall make a plausible first approximation in the present section by disregarding the rise of the surface. More exactly, we shall neglect the rise of the surface and also the squares of velocities on the surface.

To determine the potential function ψ (or ϕ), it is necessary to know boundary condition for ψ. The exact boundary condition on the free surface S of the fluid is

$$P = 0$$

(pressure is atmospheric), which by Bernoulli's equation (4.1) can be expressed in terms of the potential function ψ by

$$\frac{\partial \psi}{\partial t} = \frac{1}{2} (\text{grad}\, \psi)^2 . \tag{5.1}$$

Since this exact boundary condition is non-linear and difficult to apply, we neglect the rise of the surface S and squares of velocities on S as a first approximation. Thus, neglecting $(\text{grad}\, \psi)^2$ in (5.1) we have

$$\frac{\partial \psi}{\partial t} = 0$$

or, since the free surface S is assumed to remain at its original level,

(5.2) $\psi = 0$ on the initial plane $z = 0$ (since $\psi = 0$ at ∞).

The boundary condition (5.2) states that the impulsive pressure $\rho\psi$ is zero on the surface. This condition would be correct if the impact took place completely impulsively. Actually the time interval is very short, and so (5.2) is a good first approximation.

It is more convenient to use the potential function ϕ for unit velocity, defined by (4.4). The potential function ϕ (depending on B) satisfies the following conditions:

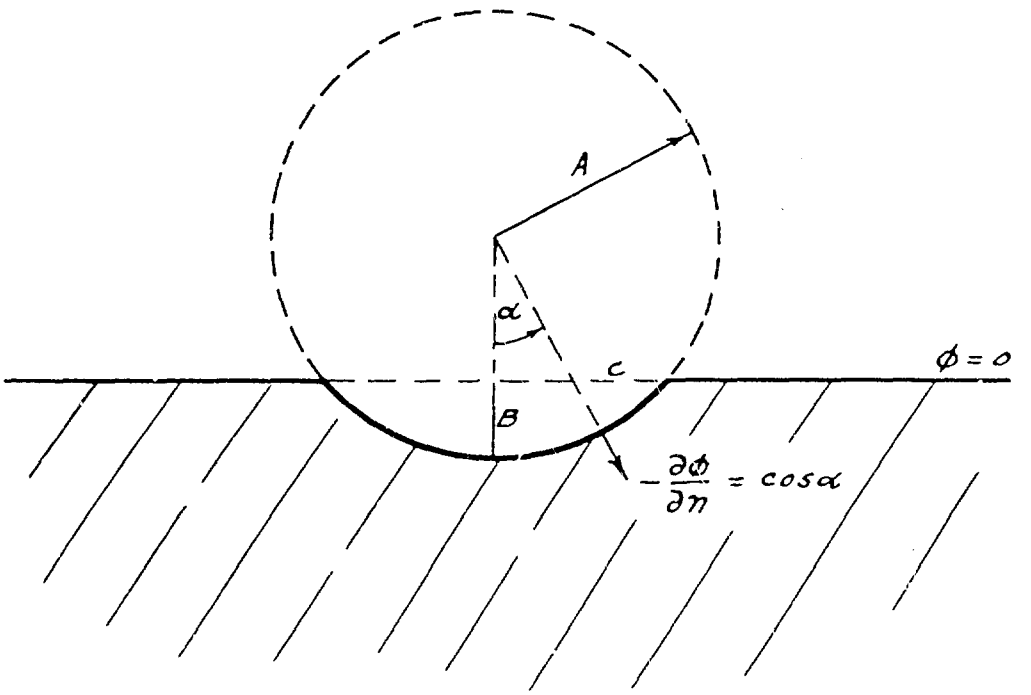

(a) On the sphere, the negative of the normal derivative of $\psi = \dot{B}\phi$ is equal to the component of the velocity of the sphere along the normal, or

$$-\frac{\partial \phi}{\partial n} = \cos\alpha \ .$$

(b) On the initial water level,

$$\phi = 0 \ .$$

There is a unique potential function satisfying these conditions.

The flow arising from the above boundary conditions has been constructed explicitly in the preceding report [15]. Because of condition (b), the potential flow can be extended to the infinite space by reflection on the surface and the flow at each instant corresponds to the steady flow about a symmetrical lens formed by the intersection of two equal

spheres. A photograph from Worthington [19] is shown below. This photograph is a view of the entering sphere from slightly

below the surface. The surface reflection creates the upper side of the lens. (Of course, the size and shape of the lens varies with time.)

The preceding report [15] supplies not only the potential function ϕ but also the corresponding virtual mass, which we shall henceforth denote by M_L, the subscript L referring to a lens. The results of [15] which we use here may be summarized as follows:

(i) The dimensionless virtual mass $m_L = \dfrac{M_L}{\frac{1}{2}\pi\rho A^3}$ is a function of b alone (where b = B/A), and will be written as $M_L(b)$. Its dependence on b is drawn in Graph 3. The impact-drag coefficient $\frac{dm_L(b)}{db}$ depends on b in the manner indicated in Graph 2. The maximum of $\frac{dm_L}{db}$ is .95 and it occurs for b = .24.

When b is small, the spherical segment beneath the initial level of the fluid is nearly a disc. By a known formula for the virtual mass M of a disc (see [8], p. 130) we therefore have

$$M = \frac{4}{3}\rho c^3$$

for B small, where c is the radius of the circle of intersection of the sphere with the original level. This gives

$$m_L(b) = \frac{M}{\frac{1}{2}\pi\rho A^3} = \frac{8}{3\pi}(2b-b^2)^{3/2}$$

or

$$m_L(b) = \frac{8}{3\pi} 2^{3/2} b^{3/2} = 2.40\, b^{3/2} \tag{5.3}$$

for small b. The more exact lens flow gives

$$\begin{cases} m_L(b) = 2.40\, b^{3/2} - 1.15\, b^2 + \cdots \\ \dfrac{dm_L}{db} = 3.60\, b^{1/2} - 2.30\, b + \cdots \end{cases} \tag{5.4}$$

(ii) The variation of the virtual mass with the depth of penetration can be better visualized by setting

$$M_L = k_L \rho c^3 , \tag{5.5}$$

where the dimensionless quantity k_L depends on b. The coefficient k_L is drawn in Graph 5. When b is small the spherical segment is nearly a disc so that

$$k_L \to \frac{4}{3} \quad \text{as} \quad b \to 0 .$$

When b = 1, the spherical segment is a hemisphere and it is then well known that $k_L = \frac{\pi}{3}$ (see [8], p. 116). The quantity k_L decreases rapidly from the value $\frac{4}{3}$ at b = 0 and then levels off, even swinging upward slightly near b = 1. This behavior of k_L is plausible on intuitive grounds. (The final coefficient k, which includes the various corrections made in this report, is also drawn in Graph 5.)

It is interesting to note that for the case of a cone instead of a sphere the quantity k is a constant independent of the depth of penetration of the cone. This results from the fact that for a cone the flow patterns at different times are geometrically similar.

To obtain a second approximation to the virtual mass and to the impact force, it is necessary to estimate the effects of the motion of the surface. On intuitive grounds, corrections due to the motion of the surface can be divided into two parts. On the one hand the water rises and wets a larger portion of the sphere, the sphere now exerting pressure on the fluid over a larger area and causing an increase in the total impact force. This will be called the "wetting" correction. On the other hand, the free surface of the fluid rises and relaxes somewhat the restraint imposed on the sphere. This will be called the "surface" correction.

These two corrections appear in formula (4.5) when written as

$$M = \rho \iint_W \phi \, dxdy + \rho \iint_S \phi \, dxdy \quad . \tag{5.6}$$

The second integral is not zero since the condition (5.1) replaces $\phi = 0$. (In fact, ϕ will turn out to be negative on S.)

Section 6. The Wetting Correction

The greatest disturbance of the surface of the fluid occurs alongside the sphere. Here a thin sheath of the fluid rises more rapidly than the rest, and may detach from the sphere (see Plate 4). This sheath because of its thinness contributes very little to the impact force (the pressure of the fluid in the sheath is practically atmospheric). The sphere exerts pressure on the fluid in the main over the portion of the sphere obtained by cutting off the thin sheath from the thick "base" of the risen fluid. This

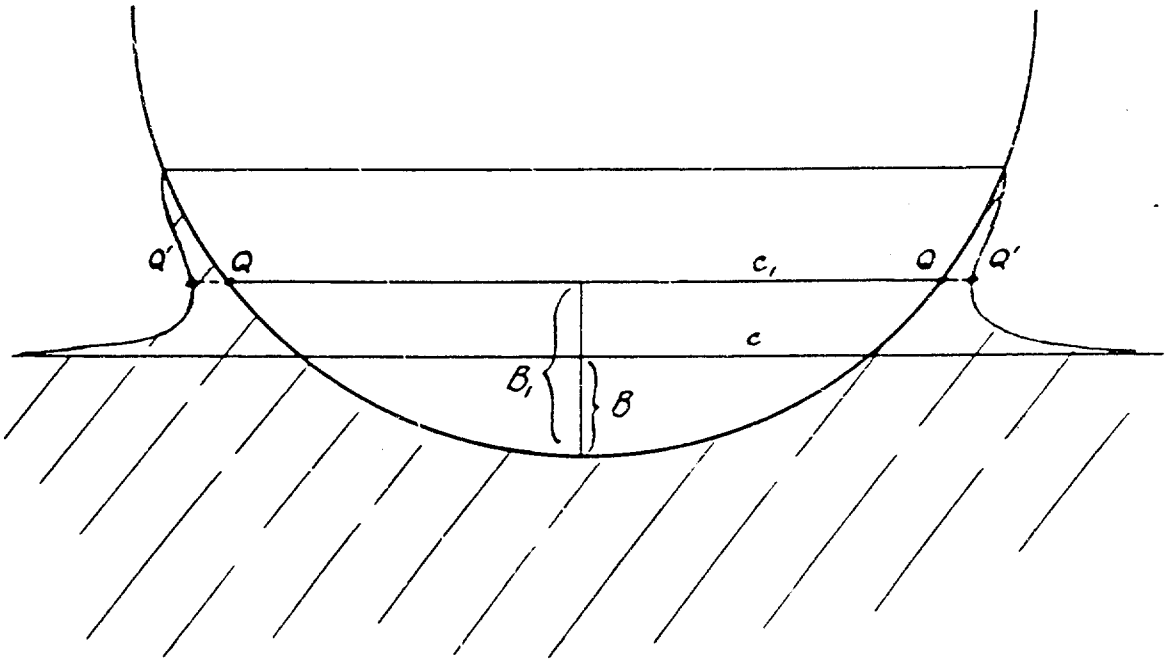

portion of the sphere is indicated by the points QQ in the diagram, and the separation of thin sheath from the thick base is indicated by the dotted lines QQ'. The flow of the fluid is due to the portion QQ of the sphere, and is approximately the flow about a lens consisting of the spherical segment QQ and a horizontal plane free surface QQ'∞ . (This may in fact be taken as the mathematical definition of the point of demarcation Q between sheath and base.)* In other words, the "base" below QQ' is so thick that its influence on the sphere is practically the same as if it extended to ∞ . It will be shown later in this section that the above discussion is exactly verified, and the definition of Q justified, in the asymptotic case as B → 0 .

---

* For the method used in the practical determination of this point of demarcation Q from photographic data, see Plate 4 and the accompanying discussion on page 23.

Henceforth it will be the spherical segment QQ which will be called the "wetted" portion W, or the "effective" portion, of the sphere. Let B_1 be the depth of this effective portion, and c_1 the radius of its circular base (see diagram). The quantity B_1 will be called the "effective depth" of penetration of the sphere. We shall also set

$$b_1 = \frac{B_1}{A} .$$

The flow of the fluid is due to the effective portion of the sphere and is approximately due to a lens with dimensions B_1, c_1 in place of B,c.

The dimensionless virtual mass $m = \frac{M}{\frac{1}{2}\pi\rho A^3}$ is given by $m_L(b_1)$ of the lens flow. Thus the dimensionless virtual mass and the drag coefficient $\frac{dm}{db}$ are

$$(6.1) \qquad \begin{cases} m = m_L(b_1) \\ \\ \frac{dm}{db} = \frac{dm_L(b_1)}{db_1} \cdot \frac{db_1}{db} \end{cases}$$

where $m_L(b_1)$ and $\frac{dm_L(b_1)}{db_1}$ are determined from the lens flow with the argument b_1.

It remains then to determine b_1 as a function of b. Set

$$(6.2) \qquad b_1 = b \cdot w(b)$$

(or equivalently, $B_1 = B \cdot w(b)$) where w(b) is a function of $b = B/A$. The quantity w(b) will be called the "wetting factor." In this section we shall show theoretically that initially, for b = 0, the wetting factor w(0) has the value 3/2. The exact dependence of w(b) on b is extremely difficult to determine

theoretically, but for small values of b the theory shows that w(b) behaves like $\frac{3}{2}$ - constant $\cdot\sqrt{b}$. Consequently, the variation of w(b) with b was determined from experimental measurements.

A blackened steel sphere of diameter 2.86 cm was dropped into a tank of water from a height of 16.2 cm and flash photographs were taken with the sphere at various stages of immersion.* The photographs in Plates 2 and 3 are a selection showing the sequences of events. Plate 4 shows an enlarged view of the splash and illustrates how the measurements were made. The straight line represents the initial surface level, the position of which was determined by a pair of inclined needles and their reflections, as indicated in the photograph. The boundary of the sphere has been completed by a white line. The exact line of demarcation between sheath and base is somewhat arbitrary but estimates can be made with a fair degree of accuracy and consistency. The upper pair of short horizontal lines shows our choice of demarcation between sheath and base. Below this line the risen water is thick while above it the water thins out very rapidly. For this particular photograph, the values of b and w(b) are:

$$b = .27$$

$$w(b) = 1.30 \quad .$$

Similar measurements were made on a number of enlarged photographs showing various depths of penetration. The quantity w(b) was then plotted against $\sqrt{b}$ with the results indicated in Graph 8(a). Also plotted in Graph 8(a) is an experimental point obtained by Watanabe while measuring impact forces. This last point is discussed in Section 9.

---

* The experiments were performed at the AMG-NYU Laboratory by M. Shamos.

The experimental points shown in Graph 8(a) fall on a reasonably well-defined straight line passing through the theoretical value w(0) = 3/2. The equation of this line is

$$w(b) = 1.5 - .4\sqrt{b} \quad . \tag{6.3}$$

In Graph 8(b), w(b) is drawn as a function of b. Actually, in Graph 8(a), the experimental points are all slightly above the straight line (6.3) near $\sqrt{b} = 1$. A more accurate curve fitting the data is the parabola

$$w(b) = 1.5 - .4\sqrt{b} + .065\, b \quad .$$

But this will make a noticeable difference only near b = 1, and we shall rather use the straight line (6.3).

It remains to derive the theoretical value w(0) = 3/2 . We shall use a method similar to one applied by Wagner [16] for the case where the entering body is a nearly flat wedge (two dimensional). In this case, the wetting factor turns out to be $\frac{\pi}{2} = 1.57$. A corresponding calculation for a very flat cone gives a wetting factor $\frac{4}{\pi} = 1.27$.

Consider the wetting correction for small b, when the sphere has entered only a small distance into the fluid. The flow of the fluid is approximately due to the spherical segment

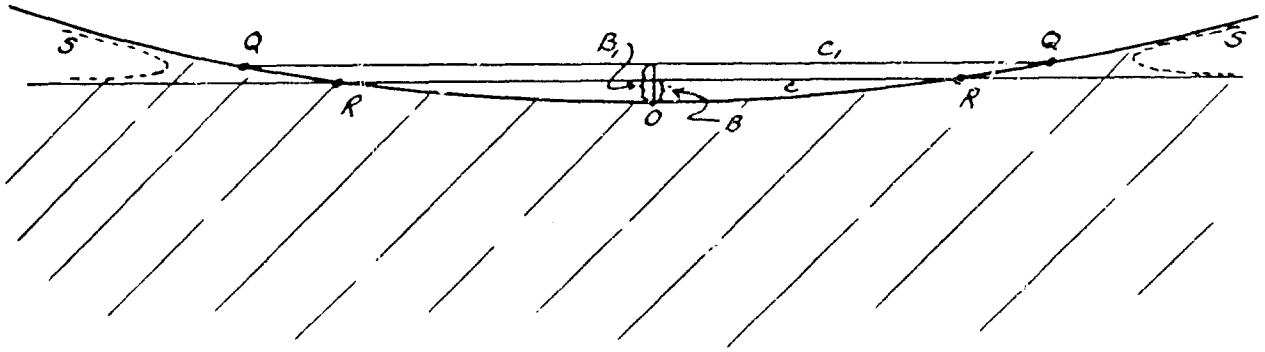

QQ. Since B and B_1 are supposed small the flow due to this spherical segment can be approximated by that due to a circular disc of radius c_1. These approximations are accurate in the limiting case as $B \to 0$, as can be seen by the following argument. Perform a similarity transformation with magnification factor $\frac{1}{c}$. The limiting situation as $B \to 0$ is indicated by the diagram below. The effective portion of the sphere

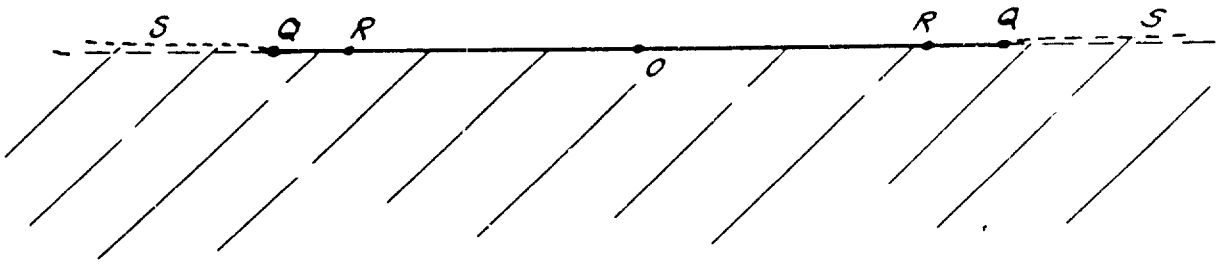

in contact with the water becomes the circular disc QQ, while the free surface becomes the plane $Q\infty$.

The theory of the flow due to a circular disc is classical ([8], pp. 130, 135, or [10], pp. 456, 457). The potential function ψ describing the flow is given in [8], p. 135. In particular the value of ψ on the lower surface of the disc is

$$\psi = \frac{2\dot{B}}{\pi}\sqrt{c_1^2 - r^2} \quad , \tag{6.4}$$

where r is the distance from the center and c_1 is the radius of the disc. The value of the upward velocity $-\frac{\partial \psi}{\partial z}$ on the free surface of the fluid, level with the disc, is ([8], p. 130):

$$-\frac{\partial \psi}{\partial z} = \frac{2\dot{B}}{\pi}\left[\frac{c_1/r}{\sqrt{1-(c_1/r)^2}} - \arcsin\frac{c_1}{r}\right] . \tag{6.5}$$

The motion of the surface of the fluid can now be followed. At any point of the free surface at distance r from the axis of symmetry, let $\eta(r)$ be the height of the free surface at the time t above its original level (the dependence of $\eta(r)$ on the time t is understood. Assume that the upward velocity of the surface at the instant t is that induced by the disc of radius c_1. From (6.5), we have

$$\dot{\eta}(r) = \dot{B} F\left(\frac{c_1}{r}\right) \tag{6.6}$$

where

$$F(\xi) = \frac{2}{\pi}\left[\frac{\xi}{\sqrt{1-\xi^2}} - \arcsin \xi\right] . \tag{6.7}$$

The quantity c_1 is a function of B_1, the relation between them depending on the shape of the incoming object. For a sphere of radius A we have

$$c_1^2 = 2AB_1 - B_1^2 . \tag{6.8}$$

For small B, (6.2) can be written as

$$B_1 = B \cdot w(0) ,$$

and (6.8) then is

$$c_1^2 = 2AB_1 = 2A\, w(0) \cdot B . \tag{6.9}$$

Thus

$$\dot{B} = \frac{c_1 \dot{c}_1}{Aw(0)} ,$$

and (6.6) becomes

$$\eta(r) = \frac{1}{Aw(0)} \int_0^{c_1} F\left(\frac{c_1}{r}\right) c_1 dc_1 . \tag{6.10}$$

(The upper limit c_1 of integration should be smaller than r. The fluid particle initially at a distance r rises until it hits the sphere, after which it enters into the thin sheath). In this integration r is kept fixed. Set

$$\frac{c_1}{r} = \xi \tag{6.11}$$

where $\xi \leq 1$. Then (6.10) becomes

$$\eta(r) = \frac{r^2}{Aw(0)} \int_0^{\xi} F(\xi)\, \xi\, d\xi \ ,$$

or, using (6.11) and (6.9),

$$\eta(r) = B \cdot \frac{2}{\xi^2} \int_0^{\xi} F(\xi)\, \xi\, d\xi. \tag{6.12}$$

Equation (6.12) represents the equation of the surface as long as $r \geq c_1$. In particular, at the position $r = c_1$, or $\xi = 1$, the height of the surface is

$$B_1 - B = B \cdot [w(0) - 1] \ .$$

Equation (6.12) yields

$$w(0) - 1 = 2 \int_0^1 F(\xi)\, \xi\, d\xi \ . \tag{6.13}$$

Substitution of (6.7) into (6.13) gives the value of the wetting factor w(0) at b = 0:

$$w(0) = \frac{3}{2} \ . \tag{6.14}$$

Evaluation of (6.12) gives the equation of the surface ~~of the~~ water

$$\eta(r) = B \cdot \frac{1}{\pi} \left[\left(\frac{3}{\xi^2} - 2\right) \arcsin \xi - \frac{3}{\xi} \sqrt{1 - \xi^2} \right] . \tag{6.15}$$

Equation (5.14) is plotted below for the case when b = .01. (Of course, this method cannot be expected to produce the thin sheath.)

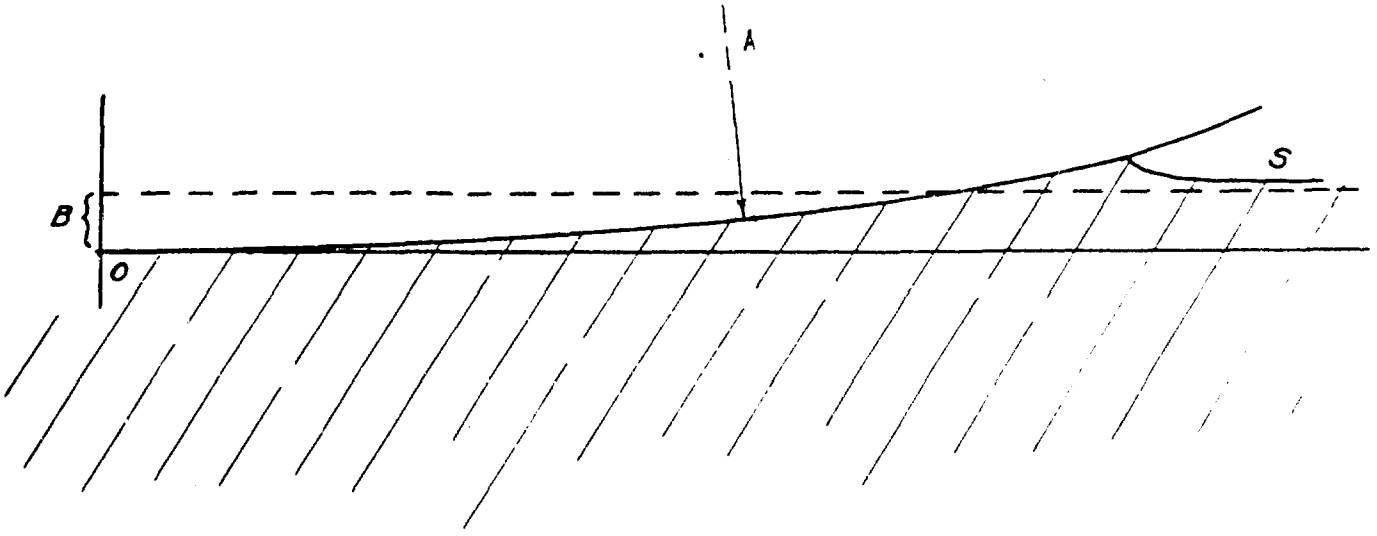

Section 7. The Free Surface Correction

The free surface correction arises from the term

$$\rho \iint_S \psi \, dxdy \tag{7.1}$$

occurring in (4.3) and the fact that we shall no longer neglect squares of velocities on S. The exact boundary condition is then

$$\frac{\partial \psi}{\partial t} = \frac{1}{2} (\text{grad}\, \psi)^2 \tag{7.2}$$

in place of $\psi = 0$ (see (5.1) and the accompanying discussion). Suppose we follow a particle of fluid on the free surface and determine the rate at which the value of ψ changes for that particle. This requires use of the "particle derivative" $\frac{D\psi}{Dt}$ where

$$\frac{D\psi}{Dt} = \frac{\partial \psi}{\partial t} - \text{grad}\, \psi \cdot \text{grad}\, \psi .$$

In view of (7.2), we have

$$\frac{D\psi}{Dt} = -\frac{1}{2}(\text{grad}\,\psi)^2 \tag{7.3}$$

on the free surface S. The value of ψ on S thus constantly decreases and is negative at any instant after the initial contact of the sphere with the fluid. This shows that the surface correction (7.1) is negative.

The correction to the impact force P arises from the time derivative of (7.1). Let the height of the surface above the initial level be

$$\eta = \eta(r,t).$$

Denote the surface correction to the impact force by P_S, so that from (4.3),

$$P_S = \rho\iint_S \frac{d\psi}{dt}\,dxdy = \rho\iint_S \left\{\frac{\partial\psi}{\partial t} + \dot{\eta}\frac{\partial\psi}{\partial z}\right\} dxdy \quad . \tag{7.4}$$

(There is no contribution from the changing domain of integration since this is cancelled by the corresponding term from $\frac{d}{dt}\left(\rho\iint_W \psi\,dxdy\right)$.) Substitution of (7.2) gives

$$P_S = \rho\iint_S \left\{\frac{1}{2}(\text{grad}\,\psi)^2 + \dot{\eta}\frac{\partial\psi}{\partial z}\right\} dxdy \quad . \tag{7.5}$$

Now assume as a reasonable approximation that the velocity on the surface S is that induced by the lens flow, used as a first approximation in Section 5. The velocity of the surface is then completely vertical, so that $\dot{\eta} = -\frac{\partial\psi}{\partial z}$ and (7.5) becomes

$$P_S = -\frac{1}{2}\rho\iint\left(\frac{\partial\psi}{\partial z}\right)^2 dxdy = -\frac{1}{2}\dot{B}^2\iint\left(\frac{\partial\phi}{\partial z}\right)^2 dxdy \quad . \tag{7.6}$$

The velocity $-\frac{\partial \phi}{\partial z}$ is infinite at the corner of the lens, but the integral (7.6) nevertheless converges. However, the integral (7.6) is a bit cumbersome to evaluate for a lens flow; we shall instead approximate the flow at each instant by that induced by an oblate spheroid circumscribing the lens. (In the previous report [5], this oblate spheroid was shown to be a reasonable approximation to the lens.)

The flow about an ellopsoid is well known (see [10], pp. 456-7) and [8], p. 132 ff.).

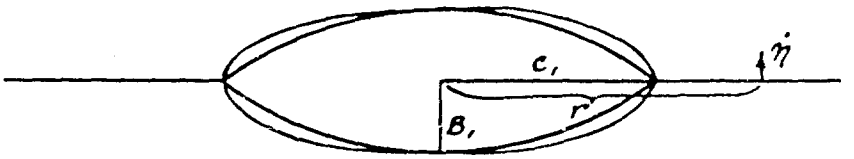

The velocity $\dot{\eta}$ on the surface is

$$\dot{\eta} = \dot{B}\,\frac{f(\xi)}{2 - f(1)}$$

where

$$f(\xi) = \frac{2\gamma}{1-\gamma^2}\left\{\frac{\xi}{\sqrt{1-(1-\gamma^2)\xi^2}} - \frac{1}{\sqrt{1-\gamma^2}}\ \text{arc sin}\ (\sqrt{1-\gamma^2}\,\xi)\right\}$$

and $\xi = \frac{c_1}{r}$, $\gamma = \frac{B_1}{c_1}$. The result of substituting this into (7.6) is

$$P_S = -\frac{1}{2}\rho \dot{B}^2 \cdot \pi A^2 \cdot K_S \qquad (7.7)$$

where

$$K_S = 2\,\frac{c_1^2}{A^2}\left\{\frac{\log(\frac{1}{\gamma}) - \frac{1-\gamma^2}{2}}{\left[\frac{\arccos\gamma}{\sqrt{1-\gamma^2}} - \gamma\right]^2} - \frac{1}{2}\right\} .$$

K_S is drawn as a function of $b = B/A$ in Graph 7. This correction is not to be considered as accurate for very small b, but should be a reasonable estimate over most of the range in which we are interested.

Section 8. The Second Approximation

The results of Sections 5,6,7 will now be collected together. Set

$$M_W = \rho \iint_W \phi \, dx\,dy ,$$

so that M_W is the contribution to the virtual mass (4.5) due to the wetted region W alone. Then equation (4.3) can be written in the form

$$P = \frac{d}{dt}\,(M_W \dot{B}) + P_s$$

where P_s is given by (7.4), or

$$P = M_W \ddot{B} + \frac{dM_W}{dB}\,\dot{B}^2 + P_s .$$

Using $M_o \ddot{B} = -P$ and (7.7), we have

$$P\left(1 + \frac{M_W}{M_o}\right) = \frac{1}{2}\rho \dot{B}^2 \cdot \pi A^2 \left\{\frac{dm_W}{db} - K_s\right\}$$

or

$$P = \frac{1}{2}\rho U_o^2 \cdot \pi A^2 \cdot \frac{\frac{dm_W}{db} - K_s}{\left(1 + \frac{M_W}{M_o}\right)\left(1 + \frac{M}{M_o}\right)^2} \qquad (8.1)$$

In this formula, the denominator can be approximated by $(1 + \frac{M}{M_o})^3$.

Comparing formula (8.1), the denominator being replaced by $(1 + \frac{M}{M_o})^3$, with formulas (3.6), (3.7), we see that

$$\frac{dm}{db} = \frac{dm_w}{db} - K_s \tag{8.2}$$

where m is the final estimate of the virtual mass, and

$$m_w = m_L(b_1) \quad .$$

Thus m may be obtained by integration, with the result

$$m = m_L(b_1) - \int_o^b K_s db \quad . \tag{8.3}$$

This is drawn in Graph 3 and compared with the first approximation $m_L(b)$ arising from the lens flow.

The impact drag coefficient is calculated from formula (3.7) using the final estimate of m. The numerator $\frac{dm}{db}$ can be written, by (8.2), in the form

$$\frac{dm}{db} = \frac{dm_L(b_1)}{db_1} \cdot \frac{db_1}{db} - K_s \quad . \tag{8.4}$$

The quantity $\frac{dm_L(b_1)}{db_1}$ may be read from Graph 2, which is a repeti-
of the result obtained in [15]; $\frac{db_1}{db}$ is obtained from formulas (6.2), (6.3); and K_s is read from Graph 7. The result for $\frac{dm}{db}$ is drawn in Graph 1 (the case $\sigma = \infty$). This is exactly the impact drag coefficient C_p in case the mass M_o of the incoming projectile is large compared to the mass of the water displaced by the hemispherical nose.

The impact drag coefficient C_p in the general case of finite σ may be calculated from formula (3.9) and the graphs of m and $\frac{dm}{db}$. The results corresponding to $\sigma = \infty$, 1, .5, .25 are shown in Graph 1.

We observe that the maximum value of C_p is about 1 (unless σ is very small), and that this maximum occurs for $b = .15$ approximately.

In the neighborhood of $b = 0$ the expansion of C_p can be obtained from (8.4), using (5.3) or (5.4). The result is

$$C_p = 6.62\, b^{1/2} - a_2 b + \dots \tag{8.5}$$

where a_2 is a coefficient which is not accurately given by (8.4) and its determination is difficult. The coefficient 6.62 is $\frac{4}{\pi} \cdot 3^{3/2}$.

In Graph 2, the final C_p is compared with the C_p obtained from the first approximation of the preceding report[15].

Section 9. Comparison with Experiment

Careful experiments on the impact of cones and spheres have been conducted by S. Watanabe (see [17]. He used a thin spherical segment, with dimensions as indicated in the diagram, on top of which were placed a weight and piezoelectric gauges connected to an oscillograph. The system was dropped from heights of 20 cm to 50 cm from the water surface, and the oscillogram record gave directly the impact force as a function of the time. The Watanabe results are exhibited in Graph 8(a),

h = ..84 cm.

Mass M_o = 1.345 kgm.

$$\sigma = \frac{M_o}{\frac{4}{3}\pi\rho A^3} = .116$$

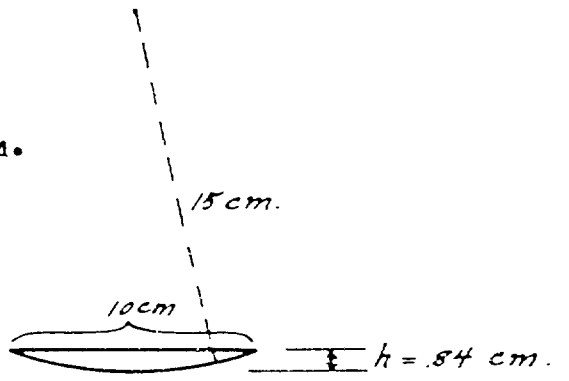

taken from his paper, the vertical axis R being the impact force measured in kilograms of force and H being the height from which the spherical segment was dropped.

These graphs are converted into graphs of C_p as follows:

$$C_p = \frac{P}{\frac{1}{2}\rho U_o^2 \cdot \pi A^2} = \frac{Rg}{\frac{1}{2}\rho \cdot 2gH \cdot \pi A^2} = \frac{R}{\pi \rho A^2 H} ,$$

$$b = \frac{\text{depth of immersion}}{A} ,$$

where the radius A of the sphere is 15 cm. The results are exhibited in Graph 8(b).

Theoretically one should expect the formula (3.9) for C_p to be valid. Expanding m and $\frac{dm}{db}$ in powers of b,

$$(9.1) \qquad \begin{cases} m = \frac{2}{3} a_1 b^{3/2} - \frac{a_2}{2} b^2 + \cdots \\ \frac{dm}{db} = a_1 b^{1/2} - a_2 b + \cdots \end{cases}$$

where a_1, a_2 are constants (from (8.3) the theoretical estimate of a_1 is 6.62. The denominator $(1 + \frac{3m}{8\sigma})^3 = 1 + \frac{9m}{8\sigma}$ near b = 0, so that

$$(9.2) \qquad C_p = \frac{a_1 b^{1/2} - a_2 b}{1 + \frac{3}{4}\frac{a_1 b^{3/2}}{\sigma} - \frac{9}{16}\frac{a_2 b^2}{\sigma}} .$$

or

$$1 = a_1 b^{1/2} \left[\frac{1}{c_p} - \frac{3b}{4\sigma}\right] - a_2 b \left[\frac{1}{c_p} - \frac{9b}{16\sigma}\right] .$$

Setting

$$y = b^{1/2}\left[\frac{1}{c_p} - \frac{3b}{4\sigma}\right] ,$$

(9.3)

$$x = b\left[\frac{1}{c_p} - \frac{9b}{16\sigma}\right] ,$$

we have

(9.4) $$a_1 y - a_2 x = 1 ,$$

The quantities y and x are plotted in Graph 9(a) using Watanabe's experimental points. They show an excellent agreement with the linear relation (9.4), and the best straight lines are likewise drawn in Graph 9(a), the resulting values of a_1 and a_2 being:

H(cm)	20	30	40	50
a_1	6.96	6.92	7.17	7.13
a_2	23.5	25.9	26.6	27.3

The values of a_1 show good agreement with the expected theoretical value 6.62.

Selecting in equation (9.2)

(9.5) $$a_1 = 6.62 ,$$

and dropping the denominator completely, we have

(9.6) $$a_2 = \frac{6.62\, b^{1/2} - c_p}{b} .$$

The quantity $\frac{6.62\, b^{1/2} - c_p}{b}$ is plotted against b in Graph 9(b), the values of b less than .01 being excluded since any experimental error in c_p will then produce a large error in a_2.

The result shows that the quantity (9.6) is accurately constant and its best value from the experimental data is 23.5. If the denominator in (9.2) is included, a correction to the value of a_2 is obtained which amounts to - 1.5. Thus, the experimental value of a_2 is

(9.7] $$a_2 = 22 \ .$$

Thus the theoretical result (9.5) is verified completely by Watanabe's experiment. In particular, the value $\frac{3}{2}$ for the wetting correction is verified.

Another more direct check of the wetting correction of $\frac{3}{2}$ is provided by Watanabe in his observation of the depth of immersion at which the resistance curve dropped sharply. The depth, in Table IV of Watanabe's paper [17], is given as .585cm on the average. This is clearly due to the water overflowing the spherical segment. The wetting factor is therefore approximately

$$w(b) = \frac{.84}{.585} = 1.44$$

which is slightly less than 3/2. The corresponding value of b is

$$b = \frac{.585}{15} = .039 \ .$$

This experimental point is plotted in Graph 6(a).

In the experiments by Blundell [3], accelerometers with low natural frequencies of 100-400 cycles/sec and low damping were used. The responses of the instruments were oscillatory,

so that only the general shape of the impact curve could be established. The dimensions of the dropped sphere are as indicated.

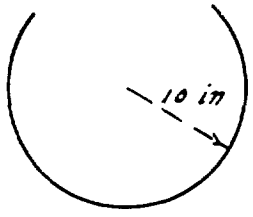

(A) M_o = 35lb, U_o = 11.4 ft/sec, σ = .23

(B) M_o = 32lb, U_o = 11.4 ft/sec, σ = .21

(C) M_o = 32lb, U_o = 8 ft/sec , σ = .21

(D) M_o = 50lb, U_o = 8 ft/sec , σ = .33

The experimental curves, obtained from Figures 1, 2 of [3]are converted into C_p curves in Graph 11(a), and the corresponding theoretical curves are drawn in Graph 11(b). An idea of the experimental error can be obtained by comparing (B) and (C), which should be the same, and by noting that (D) should give the highest C_p since σ is the largest. The agreement with theory is satisfactory, and curve (D) even agrees numerically with theory.

Richardson [13] used a hemispherical shell with the same dimensions as Blundell, but with a mass of 24 lb (σ = .159) dropped from a height of 2 ft. He used an instrument which worked on the changes in capacity of a "breathing" condenser. His experimental graph, Figure 2b of [13], is converted into the dimensionless form of a C_p curve and compared with the theoretical curve in Graph 12. The agreement is satisfacrory, especially on the position where the maximum C_p is attained.

In all these experiments, the value of σ is rather small. It is desirable to perform further experiments with a larger σ, using accurate instruments (such as piezoelectric gauges).

Appendix

Section 10. Comparison of Energy and Momentum

In Sections 3 and 4 the force of impact was derived from momentum considerations, and we found that the force on the entering sphere is equal to the time rate of change of the resultant impulsive pressure force acting on the boundary of the fluid (formula (4.3)). We may, however, derive the force of impact from energy considerations.

Let $\frac{1}{2} M_e U^2$ be the kinetic energy of the fluid at time t, where M_e is the "energy" virtual mass. By the principle of conservation of energy, we have

$$(10.1) \qquad \frac{1}{2}(M_e + M_o) U^2 = \frac{1}{2} M_o U_o^2 \quad , \text{ or } \quad U^2 = \frac{U_o^2}{1 + \frac{M_e}{M_o}} .$$

Differentiating with respect to t and using (3.2), we obtain

$$(10.2) \qquad P = \frac{1}{2} \frac{\frac{dM_e}{dB}}{1 + \frac{M_e}{M_o}} U^2 = \frac{1}{2} \frac{\frac{dM_e}{dB}}{(1 + \frac{M_e}{M_o})^2} U_o^2$$

by (10.1).

Formulas (10.1), (10.2) should be compared with the corresponding formulas (3.3), (3.4) based on momentum considerations. An immediate comparison of (10.1) and (3.3) shows that

$$(10.3) \qquad 1 + \frac{M_e}{M_o} = (1 + \frac{M}{M_o})^2 \text{ or } M_e = 2M(1 + \frac{1}{2}\frac{M}{M_o})$$

where M is the "momentum" virtual mass which we have been using throughout. The same relation is obtained by comparing (10.2) and (3.4). For incoming projectiles of large mass compared to the mass of the water displaced by the hemispherical nose, $\frac{1}{2} M/M_0$ is small compared to 1, and we have approximately

$$M_e = 2M . \tag{10.4}$$

Thus, for impact, M_e is different from M.

In order to obtain an expression for M_e, we observe that the total kinetic energy of the fluid is

$$\frac{1}{2} M_e U^2 = \frac{1}{2}\rho\iiint (\text{grad}\,\psi)^2 \, dxdydz = -\frac{1}{2}\rho\iint \psi \frac{\partial \psi}{\partial n} \, dS - \frac{1}{2}\rho\iint \psi \frac{\partial \psi}{\partial} \, dS$$

by Green's theorem, where the differentiation is with respect to the normal pointing into the fluid.* Thus the kinetic energy is equal to the work done by the impulsive forces acting on the boundary of the fluid. Since $-\frac{\partial \psi}{\partial n} = U \cos\alpha$ on W (see diagram on page 17), we see that $-\frac{\partial \psi}{\partial n} dS = U \, dxdy$. Substituting from (4.4), we therefore obtain for M_e the formula

$$M_e = \rho\iint_W \phi \, dxdy + \rho\iint_S \phi \left(-\frac{\partial \phi}{\partial n}\right) dS \quad . \tag{10.5}$$

Comparing the right hand sides of (10.5 and (4.6), we see that they differ only in their second terms, the free surface terms. If the same first approximation is made as previously, that is $\phi = 0$ on the surface, we would obtain

$$M_e = \rho\iint_W \phi \, dxdy = M$$

* It is easily seen (from the considerations of Section 4) that the integration extended over a large spherical membrane tends to zero as the membrane tends to infinity.

whereas we know that $M_e = 2M$ approximately. The complete neglect of the surface terms may thus cause a sizeable error amounting to the factor 2.

We shall show that the neglect of the surface term is justifiable when momentum is used and not justifiable when energy is used. The reason for this is that the rapidly rising fluid immediately surrounding the sphere carries considerable energy but not much momentum. This portion of the fluid includes the thin sheath and the thick base of the surface rise adjacent to the sphere, all of which will be grouped together and called the splash. We may thus think of the splash as carrying the energy which would normally be dissipated into heat in inelastic impact.

We shall show that the percentage of energy carried by the splash is much larger than the percentage of momentum carried by it, at least for the depths of penetration in which we are interested. This is plausible on intuitive grounds since the mass of the splash is concentrated near the sides of the sphere and is moving outward as well as upward (see Plate 5). The outward or horizontal motion of the splash contributes to the kinetic energy, but contributes nothing to the momentum because of the rotational symmetry about the vertical direction.*

At each instant, the additional water entering the splash is shed off the side of the sphere at the place where the water level intersects the sphere. Let u_h and u_v be the horizontal and vertical components of the splash as it leaves the sphere, and let θ be the angle indicated in the diagram. The velocity with which the splash is moving in the direction normal to the sphere is $U \cos \theta$, where U is the vertical velocity of the

---

* This remark is not valid in the case of oblique entry. Because of the asymmetry there is then a sizable horizontal component of the momentum of the splash.

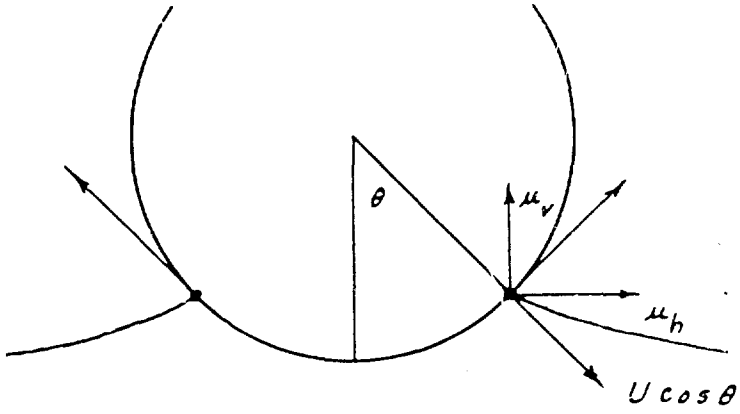

sphere. We therefore have (see the diagram)

$$u_h = (u_v + U)\cot\theta$$

and so the magnitude u of the resultant splash velocity is given by

$$u = u_v\sqrt{1 + (1 + \frac{U}{u_v})^2 \cot^2\theta} \ .$$

Let M be the virtual mass of the water defined in Sections 3, 4. By (10.4), $M_e = 2M$ and so the total kinetic energy of the fluid is $\frac{1}{2}M_eU^2 = MU^2$. Hence, if m_{sp} is the mass of water entering the splash, the fraction of the energy carried by the splash is

$$(10.6) \qquad \frac{\frac{1}{2}m_{sp}u^2}{MU^2} = \frac{1}{2}\frac{m_{sp}}{M}(\frac{u_v}{U})^2\left[1 + (1 + \frac{U}{U_v})^2\cot^2\theta\right] .$$

The total momentum of the splash is directed virtually upward by rotational symmetry and is equal to $m_{sp}u_v$. Dividing by the effective momentum MU of the fluid we obtain

$$(10.7) \qquad \frac{m_{sp}u_v}{MU} = \frac{m_{sp}}{M} \cdot \frac{u_v}{U}$$

for the fraction of the momentum carried by the splash.

The ratio of (10.6) to (10.7) is

$$(10.8) \qquad \frac{\text{percentage energy in splash}}{\text{percentage momentum in splash}} =$$

$$\frac{1}{2}\frac{u_v}{U}\left[1 + \left(1 + \frac{U}{u_v}\right)^2 \cot^2\theta\right] \geq \frac{1}{\sec\theta - 1}$$

for any $\frac{u_v}{U}$. The following table exhibits the minimum values of the ratio (10.8) for various angles θ:

θ	0°	15°	30°	45°	60°	75°	90°
minimum possible value of ratio (10.8)	∞	28.3	6.5	2.4	1	.35	0

This table gives the minimum value of the ratio (10.8) as the fluid is shed off into the splash. The ratio (10.8) for the total splash is some sort of integral of $\frac{1}{\sec\theta - 1}$. Thus, in the early stages of the entry of the sphere the energy loss in the splash is much greater than the momentum loss. For this reason, an approximation based on momentum is more accurate than one based on energy.

In Sections 7, 8 of the present report, we have computed the correction to the virtual mass M due to the motion of the surface. The surface correction to the dimensionless virtual mass m is $\int_0^b K_s db$. This correction exhibits the behavior indicated above. At the beginning, near b = 0, the correction is relatively small. The relative magnitude of the correction increases until near b = 1 it amounts to about 20 percent.

From the mathematical side we can see why the surface correction is smaller on a momentum basis than on an energy basis. The surface correction, on a momentum basis, is merely $\rho\iint_S \phi \, dxdy$. On an energy basis the surface correction is by (10.5) $\rho\iint_S \phi \left(-\frac{\partial\phi}{\partial n}\right) dS$ which has the extra factor $\frac{\partial\phi}{\partial n}$. The surface of the water immediately adjacent to the sphere is moving up rapidly, so that $\frac{\partial\phi}{\partial n}$ is large there and $\rho\iint_S \phi(-\frac{\partial\phi}{\partial n})dS$ is larger than $\rho\iint_S \phi \, dxdy$.

Also, since the surface is rising, $-\frac{\partial\phi}{\partial n}$ is negative (n is the inward pointing normal) and so $\rho\iint_S \phi(-\frac{\partial\phi}{\partial n})dS$ is positive, remembering that ϕ is negative on the free surface. Thus

$$M > \rho\iint_W \phi \, dxdy < M_e \quad ,$$

the inequalities being due to the surface terms.

BIBLIOGRAPHY

[1] Bell, G. E., "On the impact of a solid sphere with a fluid surface," Phil. Mag., Vol. 48 (1924), pp. 753-764. [Effect of viscosity of the fluid and various surface coatings of the sphere on the surface disturbance and shape of the cavity.]

[2] Birkhoff, G., Birkhoff, G. D., Bleick, W., Handler, E., Murnaghan, F., Smith, T., "Ricochet off water," AMP Memo 42.4M, AMG-C No. 157 (1944).

[3] Blundell, R. W., "Force measurements on a hemisphere when dropped into water," Marine Aircraft Establishment, Felixstone, M.A.E.E. Report No. F/Res/106 (1937).

[4] Davies, R. M., "The influence of atmospheric pressure on the phenomena accompanying the fall of small scale projectiles into a liquid," Engineering Laboratory, Cambridge, U.B.R.C. No. 21 (Sept., 1944). [The effect of atmospheric pressure on the cavity and its closure.]

[5] Jones, A. T., "The sounds of splashes," Science, N.S. 52 (1920), pp. 295-296. [Discusses sounds made by drops falling on a fluid surface. Heights of fall corresponding to silent drops separated by heights at which sound is produced.]

[6] Krebs, R. L., "Experimental investigation of impact in landing on water," N.A.C.A. Technical Memorandum No. 1046 (August, 1943).

[7] v. Karman, Th., "The impact on seaplane floats during landing," N.A.C.A. Tech. Note No. 321 (1929).

[8] Lamb, H., Hydrodynamics, Cambridge University Press (Fifth Ed., 1924).

[9] Mallock, A., "Sounds produced by drops falling on water," Proc. Roy. Soc., A, Vol. 95 (1919) pp. 138-143. [Investigates musical notes produced by drops falling on liquid surface. Approximate calculation of shape of cavity.]

[10] Milne-Thompson, "Theoretical Hydrodynamics," MacMillan (1938)

[11] Pabst, W., "Theorie des Landestosses von Seeflugzeugen," Zeitschrift für Flugtechnik und Motorluftschiffahrt (1930), pp. 217-226. [Obtains virtual mass corresponding to rectangular plate by comparing periods of oscillation in air and water.]

[12] Raman, C. Y., and Dey, A., "On the sound of splashes," London, Edinborough and Dublin Phil. Mag., 5.6 Vol.39, No. 229 (Jan., 1920), pp. 145-147. [Discusses records of sounds produced by drops falling on liquid surface.]

[13] Richardson, E. G., "Impact on Water: A Summary," U.B.R.C. No. 30 (Jan. 4, 1945).

[14] Sedov, L., "The impact of a rigid body gliding on the surface of an incompressible fluid," Works of the Central Aerohydrodynamical Institute, No. 187, Moscow (1934). [General theoretical discussion of impact on a water surface and detailed treatment of two-dimensional problem of oblique impact of a rotating elliptic cylinder.]

[15] Shiffman, M., and Spencer, D. C., "The force of impact on a sphere striking a water surface," AMP Report 42.1R, AMG-NYU No. 105 (1945).

[16] Wagner, H., "Über Stoss- und Gleitvorgänge an den Oberflächen von Flüssigkeiten," Zeitschrift für angewandten Mathematik und Mechanik, Vol. XII, No. 4, pp. 193-215.

[17] Watanabe, S., "Resistance of impact on water surface; Part V-Sphere," Scientific Papers, Institute of Physical and Chemical Research, Tokio, Vol. 23, No. 484 (1933) pp. 202-209.

[18] Watanabe, S., "Resistance of impact on water surface; circular plane, sphere and cylinder," Proc. 4th Int. Congr. App. Mech., Cambridge (1934), pp. 265-266.

[19] Worthington, A. M., "A Study of Splashes," Longmans, Green and Co., London (1908). [Description of phenomena produced by liquid drops and solid spheres falling on a liquid surface. Many excellent photographs.]

[20] Worthington, A. M., and Cole, R. S., "Impact with a liquid surface," Phil. Trans. Roy. Soc., A, Vol. 189 (1897), pp. 137-148, and A. Vol. 194 (1900), pp. 175-200. [Detailed discussion of experiments performed in studying phenomena produced by spheres falling in water.]

[21] Proceedings of the Second Conference on Underwater Ballistics, AMP, AMG-H (1945). [A complete summary of recent work on underwater ballistics.]

Graph 1 Impact Drag Coefficient

$$C_p = \frac{\frac{dm}{db}}{\left(1 + \frac{3m}{8\sigma}\right)^3}$$

where σ = mass of incoming projectile $\frac{4}{3}\pi\rho A^3$

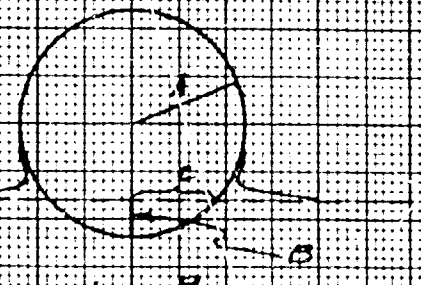

C_p

1.00
.80
.60
.40
.20
0

$r = 8$
$r = 1.0$
$r = 0.5$
$r = 0.25$

.1 .2 .3 .4 .5 .6 .7 .8 .9 1.0

$b \rightarrow$

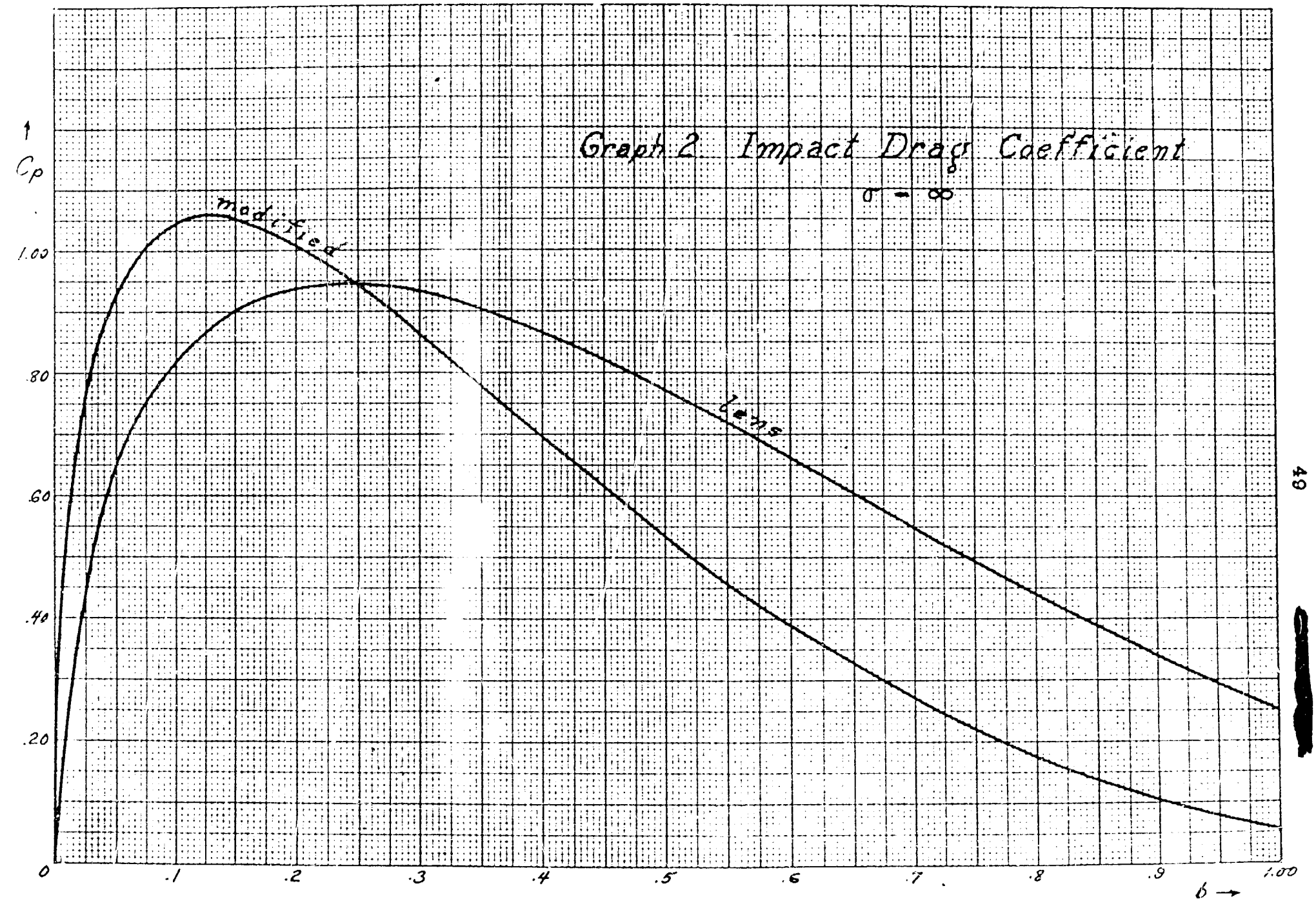
Graph 2 Impact Drag Coefficient
σ → ∞
Cp
1.00
.80
.60
.40
.20
0
.1
.2
.3
.4
.5
.6
.7
.8
.9
1.00
b →
modified
Lens

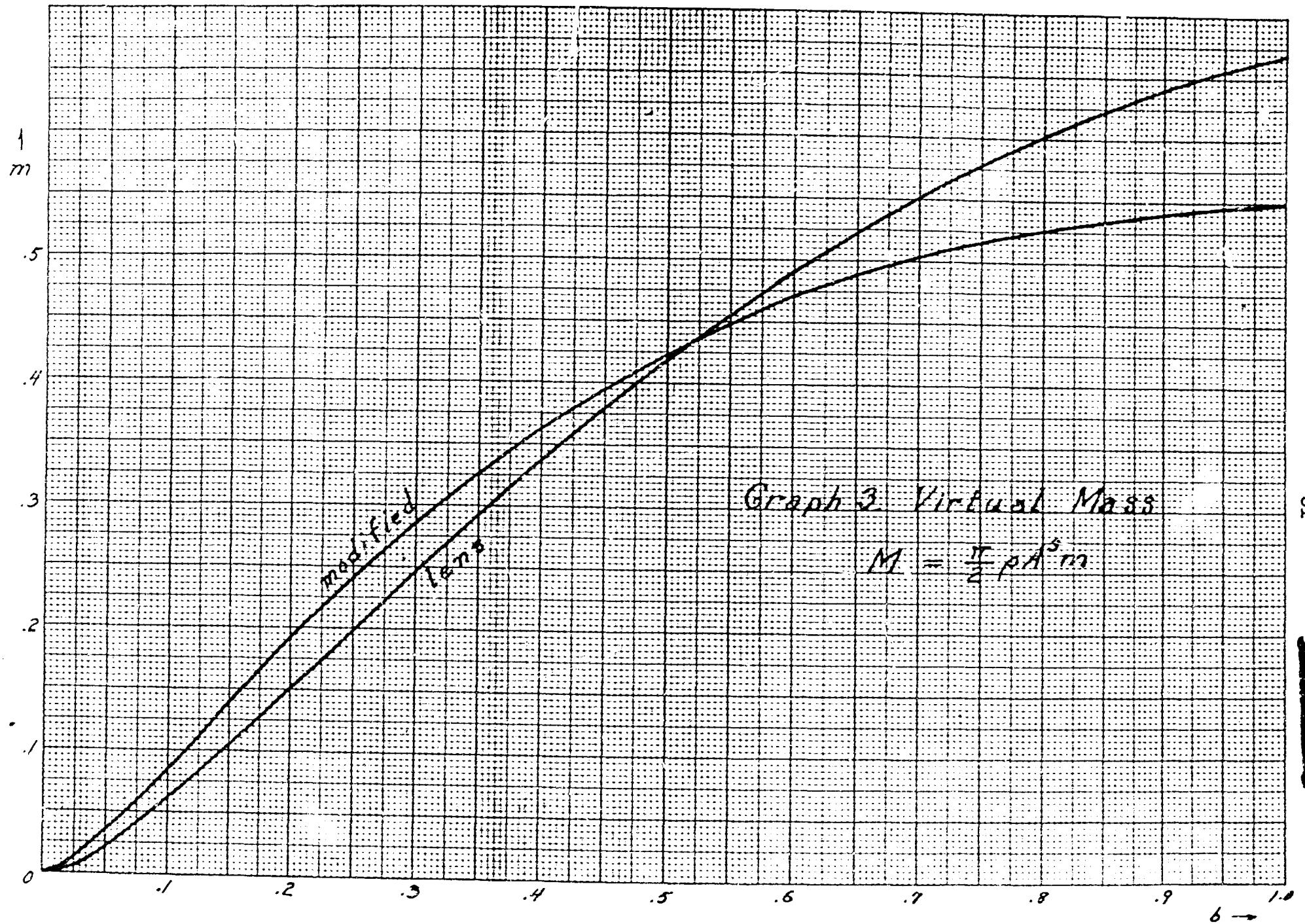

Graph 3 Virtual Mass

$$M = \frac{\pi}{2} \rho A^2 m$$

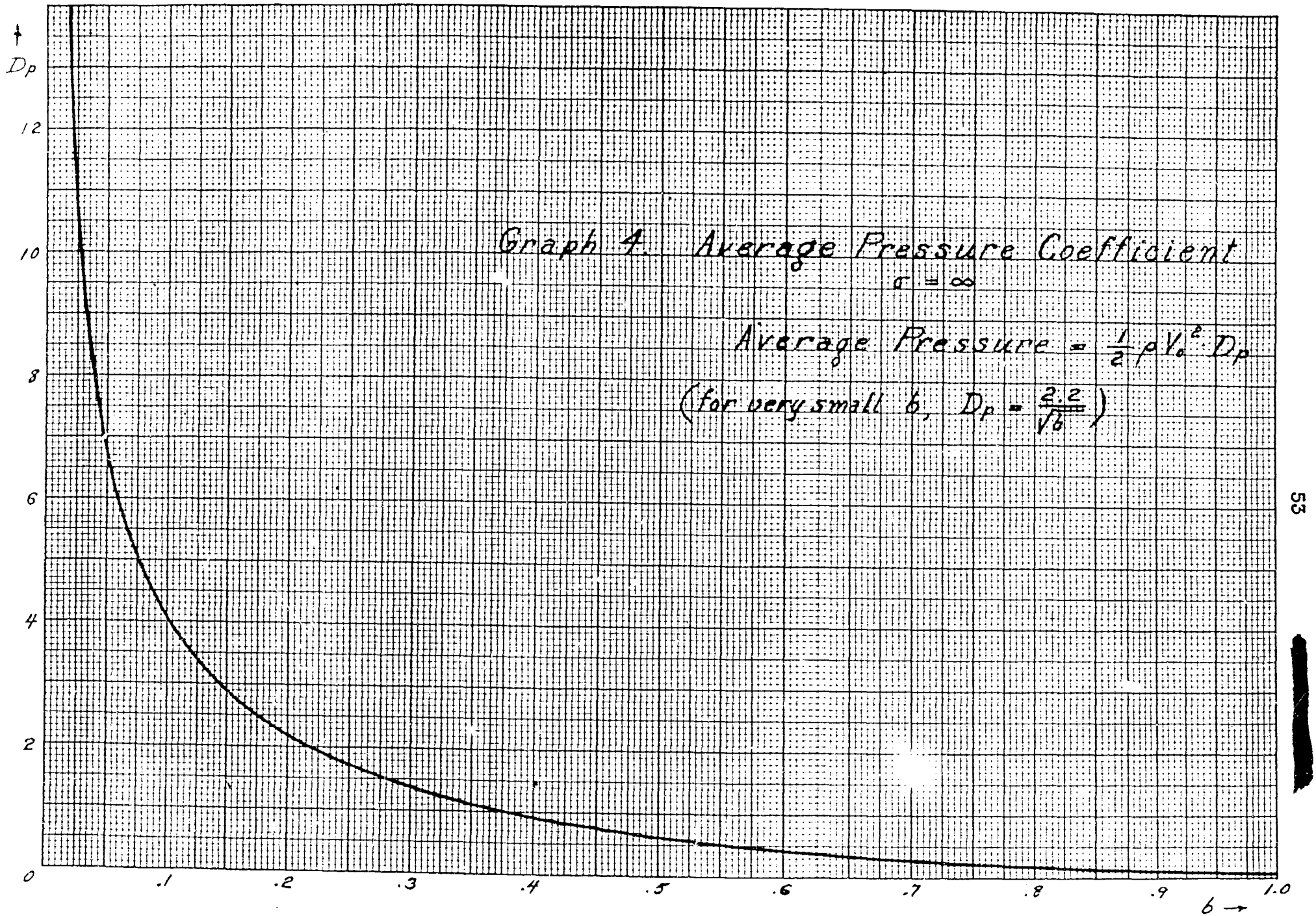

Graph 4. Average Pressure Coefficient

$\sigma = \infty$

Average Pressure $= \frac{1}{2} \rho V_0^2 D_p$

(for very small b, $D_p = \frac{2.2}{\sqrt{b}}$)

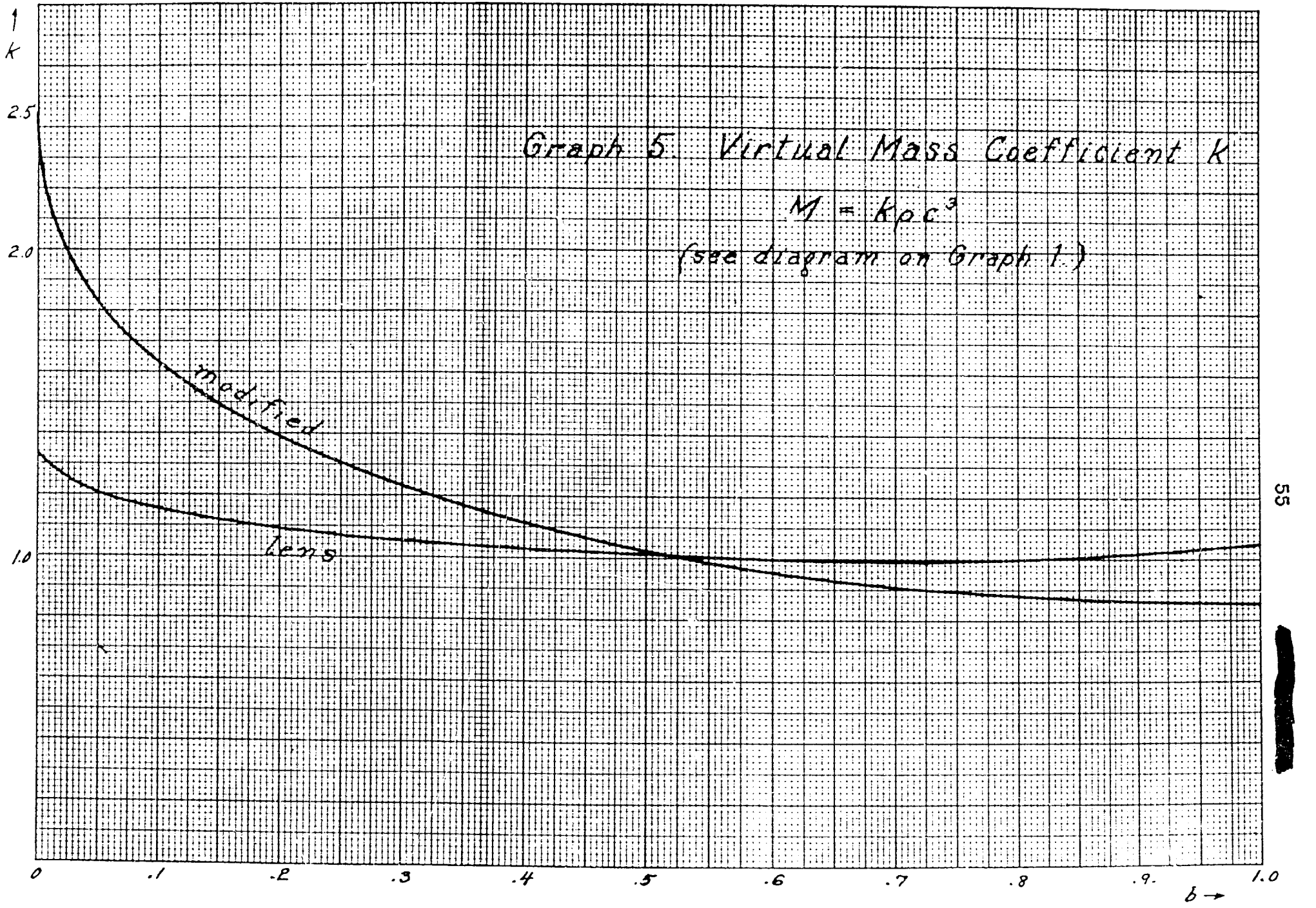
K
2.5
2.0
1.0
Graph 5. Virtual Mass Coefficient K
M = Kρc³
(see diagram on Graph 1.)
modified
lens
0
.1
.2
.3
.4
.5
.6
.7
.8
.9
1.0
b →

Graph 6. Wetting Factor

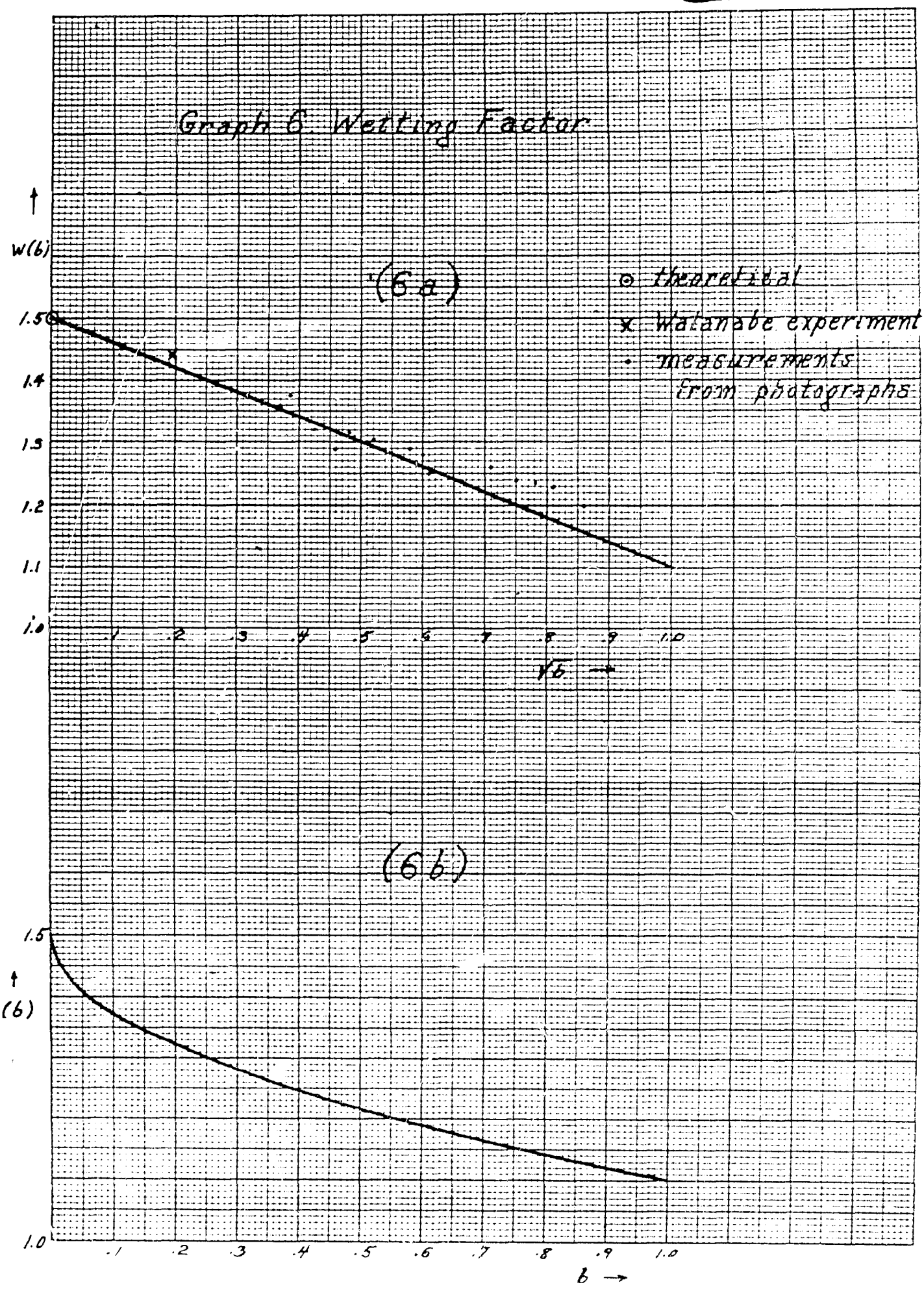

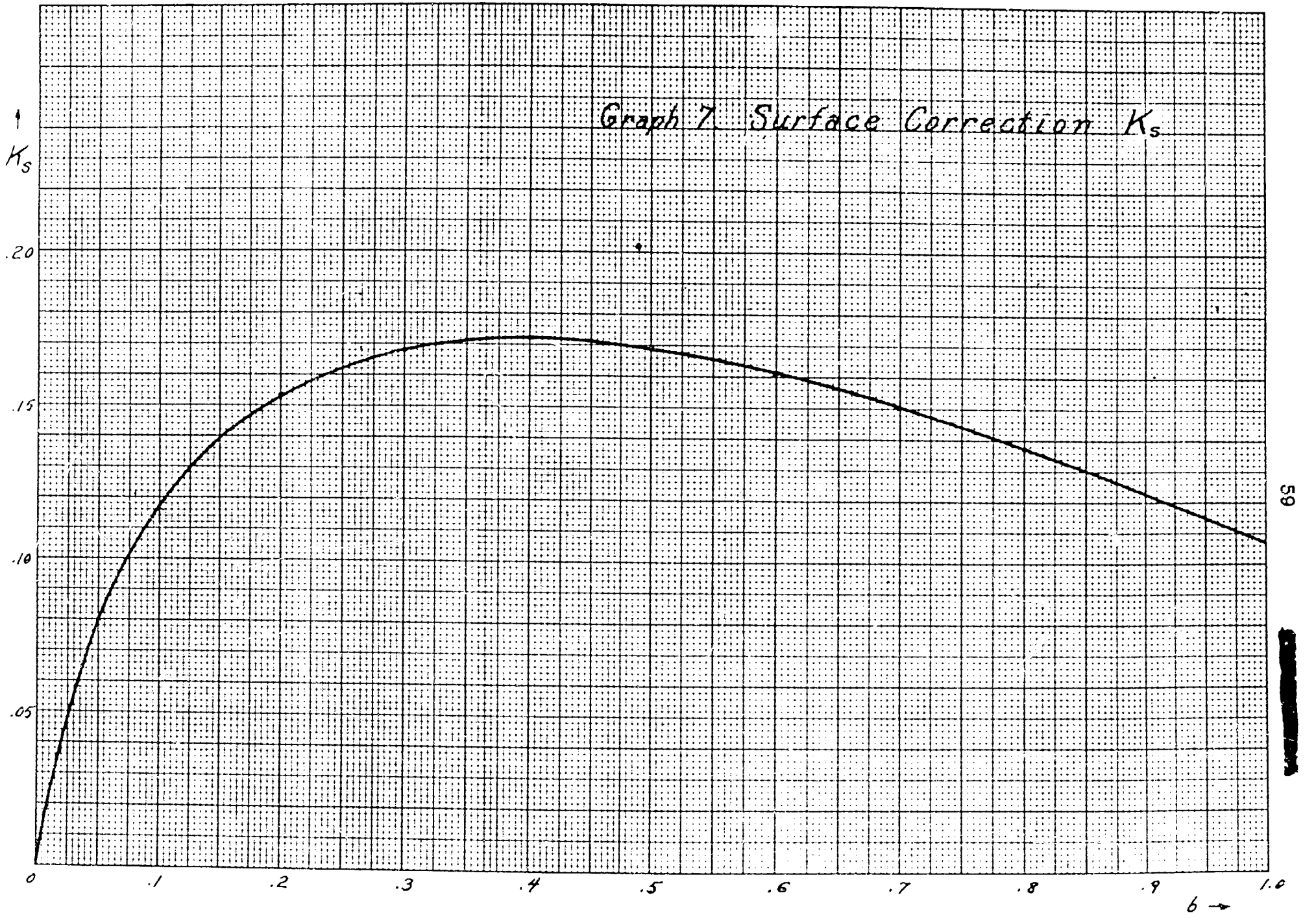
Graph 7 Surface Correction K_s
K_s
.20
.15
.10
.05
0
.1
.2
.3
.4
.5
.6
.7
.8
.9
1.0
δ →

Graph 8. Watanabe Experiments

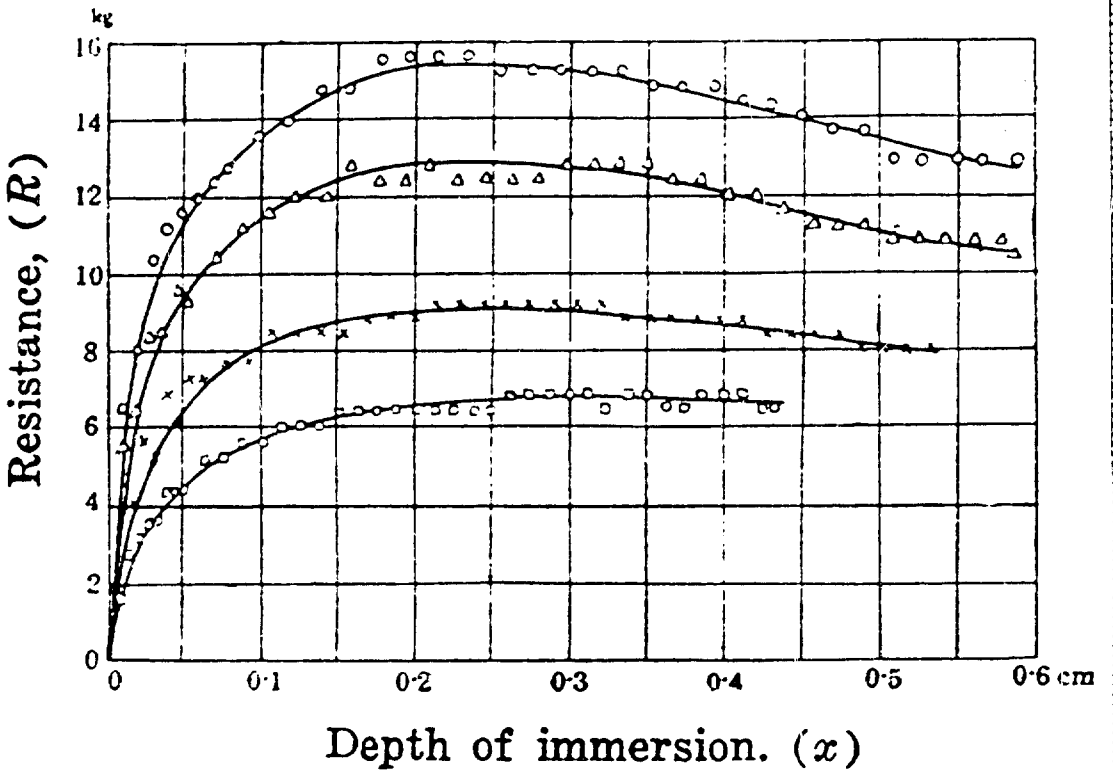

8(a)

○ H = 51 cm
△ " 41 "
× " 31.2 "
□ " 20 "

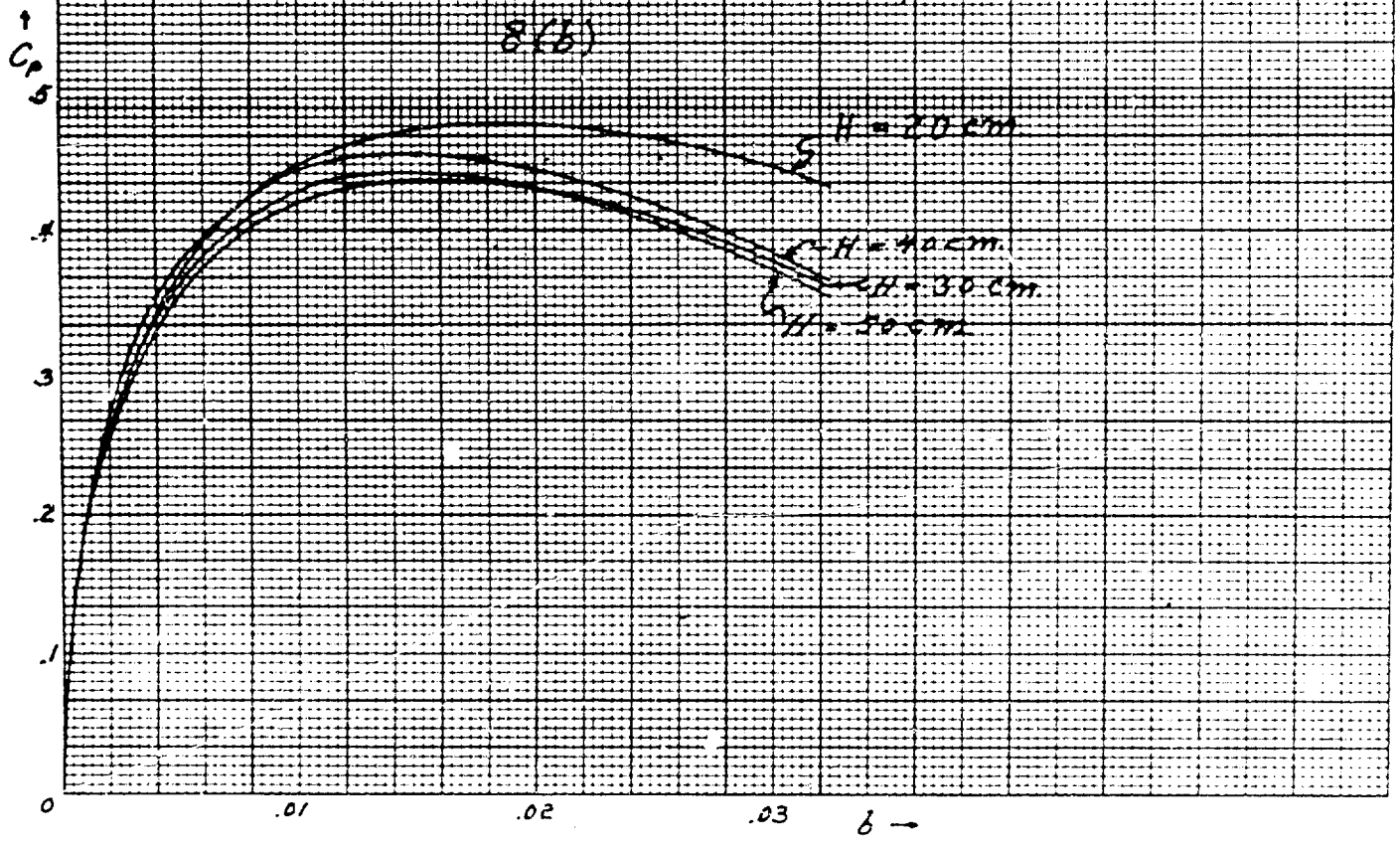

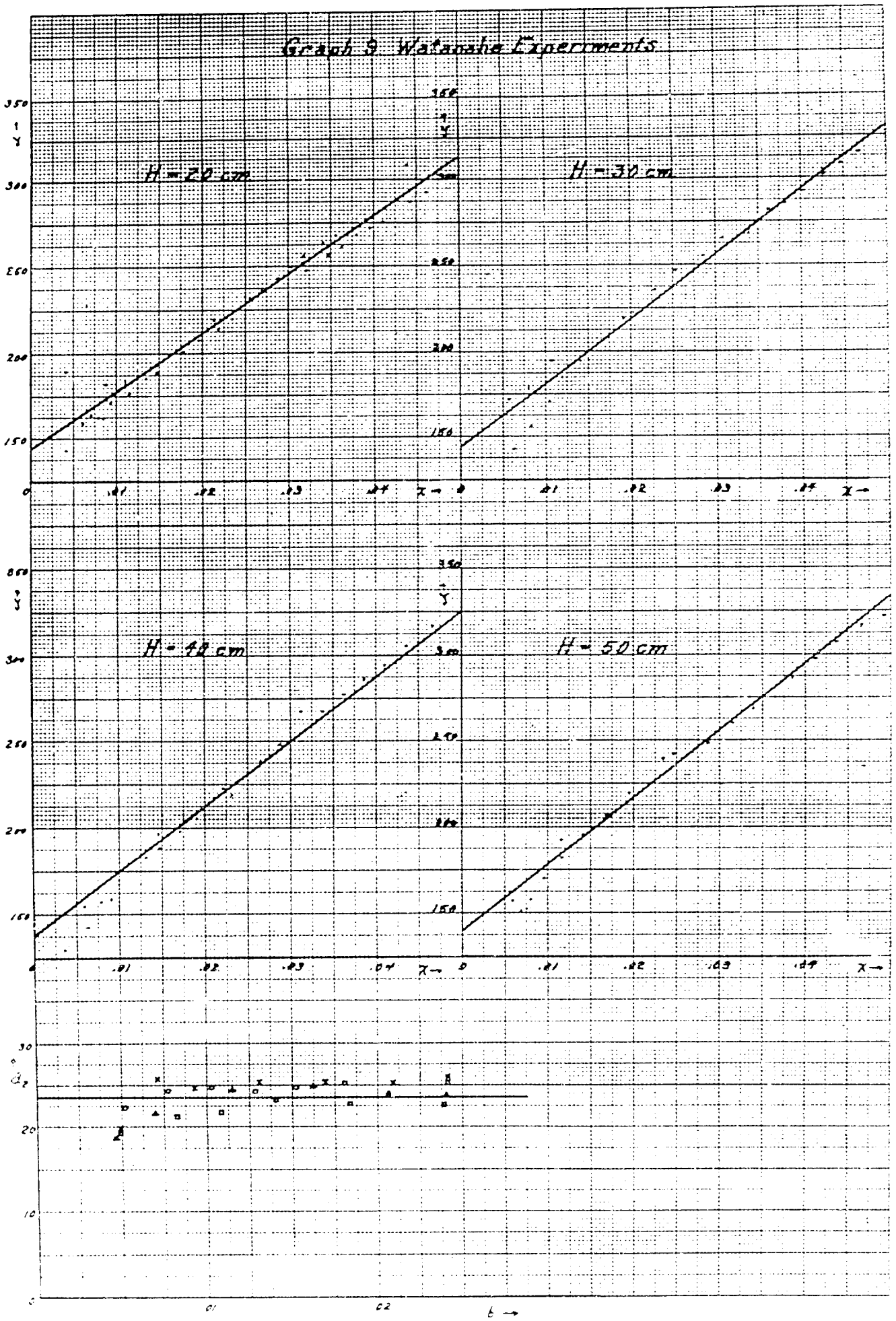
Graph 9 Watanabe Experiments
H = 20 cm
H = 30 cm
H = 40 cm
H = 50 cm
Y
X →
350
300
250
200
150
0
.01
.02
.03
.04
30
20
10
α_2
β →

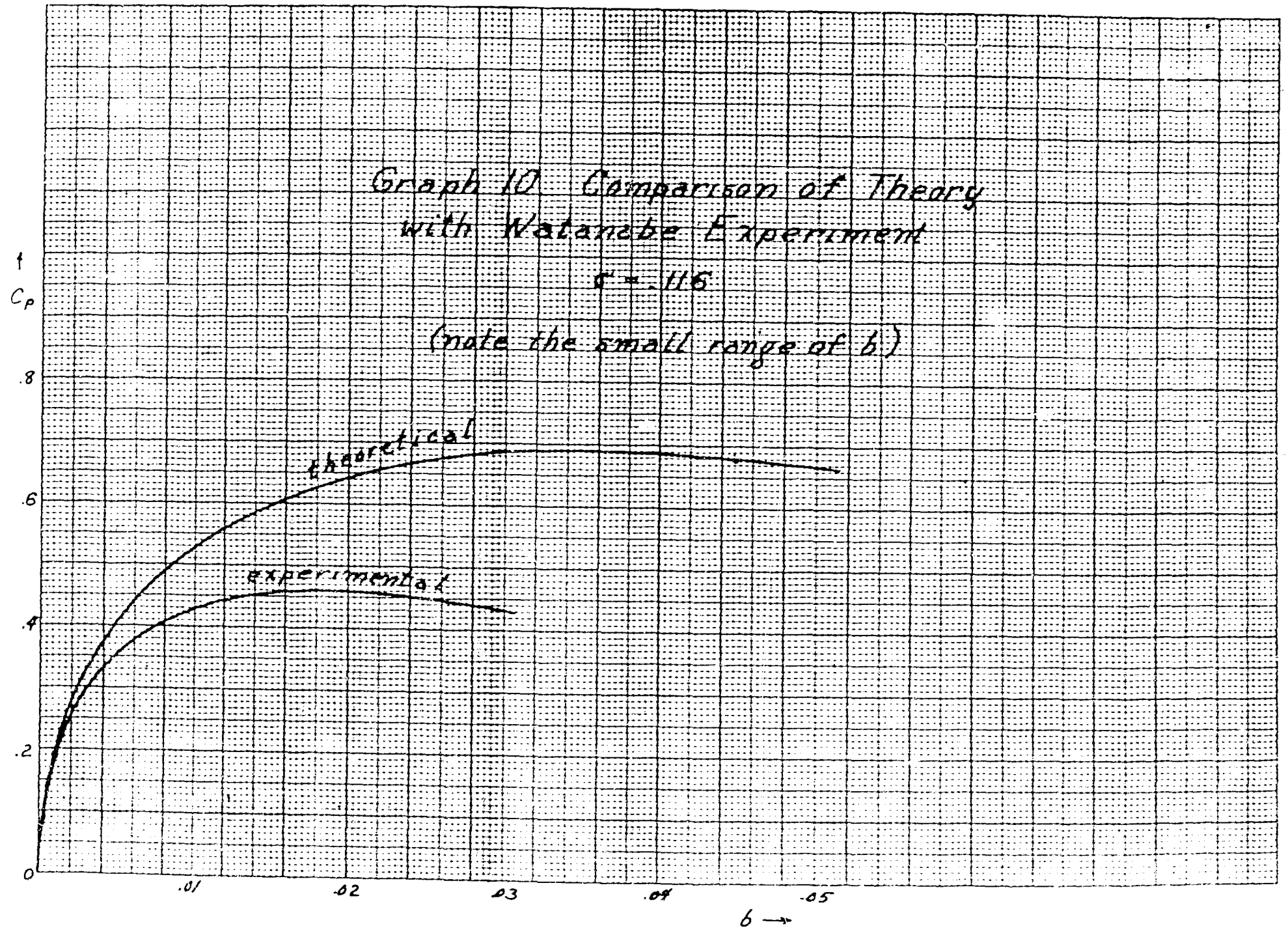
Graph 10 Comparison of Theory
with Watanabe Experiment
$\sigma = .116$
(note the small range of b)
C_p
.8
.6
.4
.2
0
theoretical
experimental
.01
.02
.03
.04
.05
b →

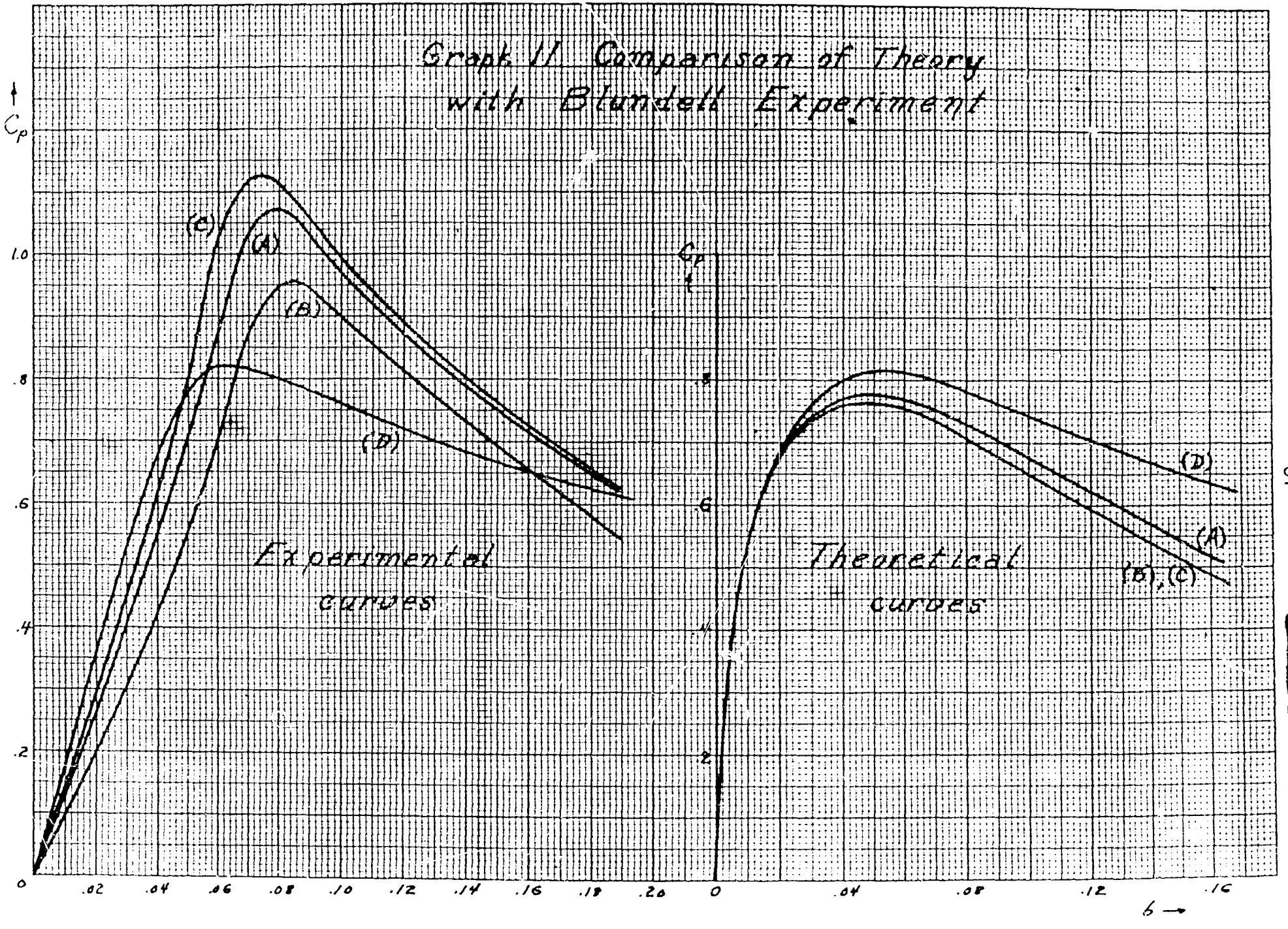
Graph II Comparison of Theory with Blundell Experiment
C_p
1.0
.8
.6
.4
.2
0
.02
.04
.06
.08
.10
.12
.14
.16
.18
.20
(C)
(A)
(B)
(D)
Experimental curves
C_p
.8
.6
.4
.2
0
.04
.08
.12
.16
(D)
(A)
(B), (C)
Theoretical curves
$\delta \rightarrow$

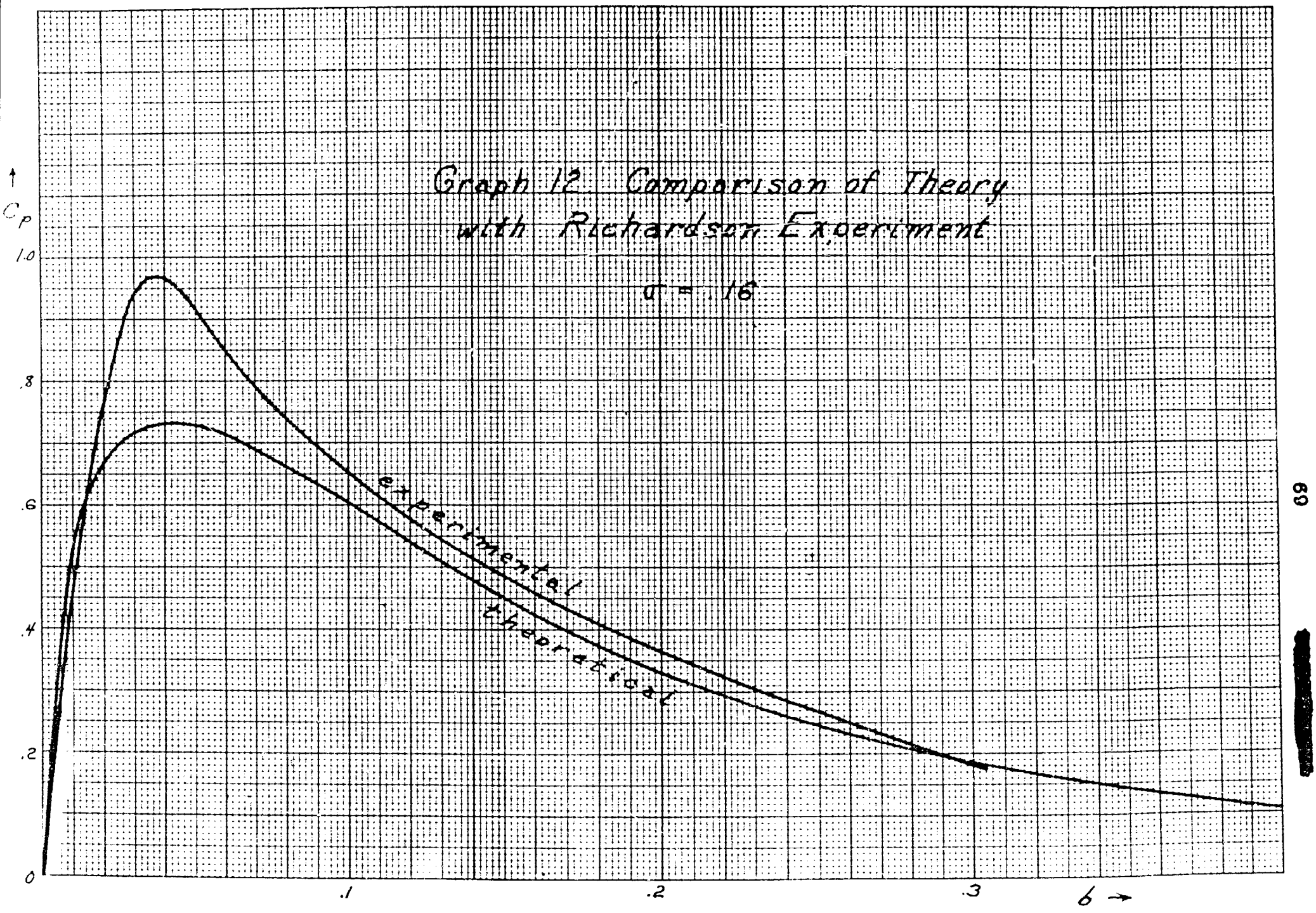
Graph 12 Comparison of Theory
with Richardson Experiment
σ = 16
C_p
1.0
.8
.6
.4
.2
0
.1
.2
.3
δ →
experimental
theoretical

Polished serpentine sphere falling 14 cm. into water.

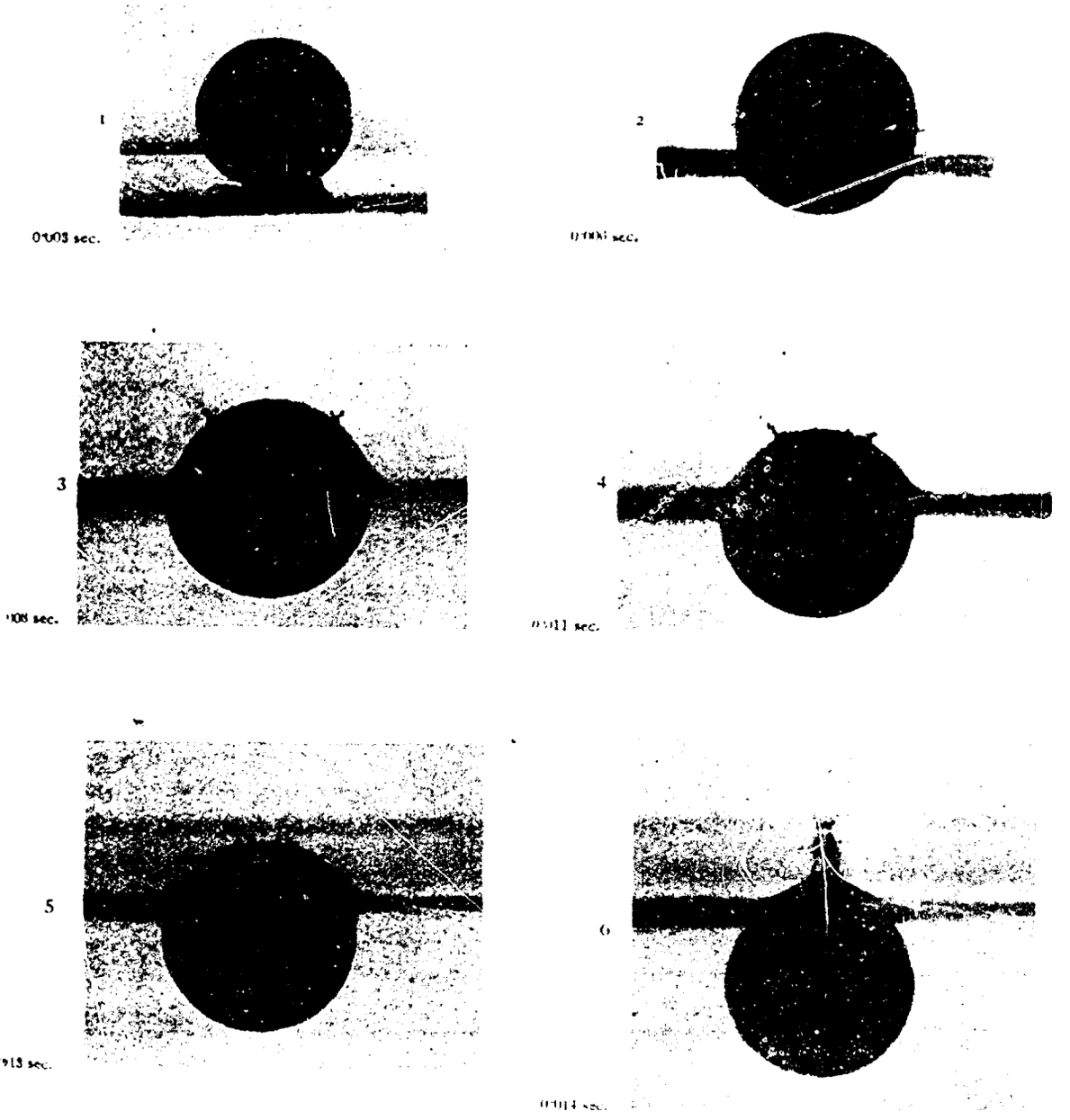

This plate is taken from A. M. Worthington, "A Study of Splashes", 1908.

Plate 1

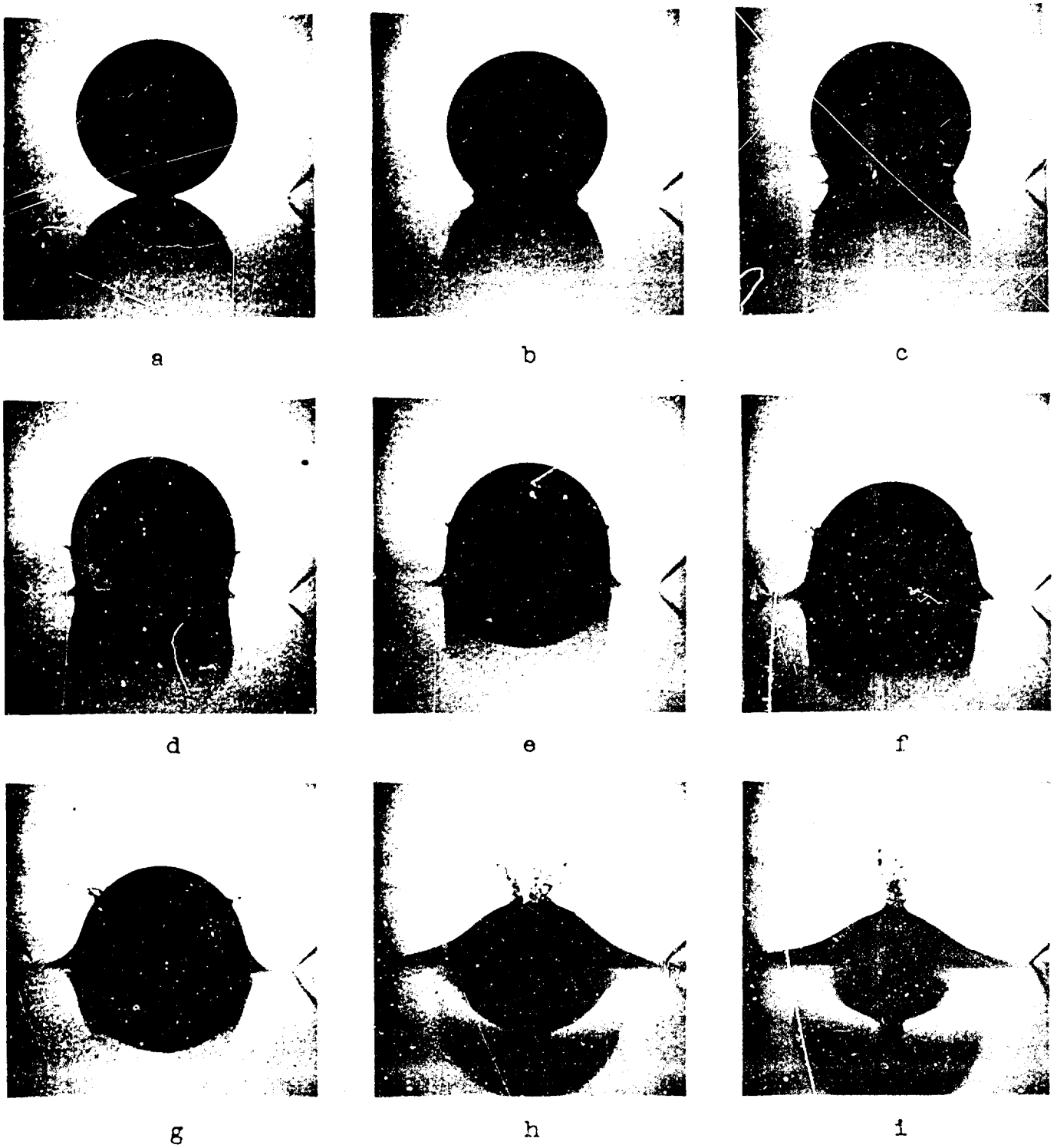

a b c

d e f

g h i

SMOOTH ENTRY

Steel sphere of diameter 2.86 cm. dropped from a height of 16.2 cm.

Plate 2

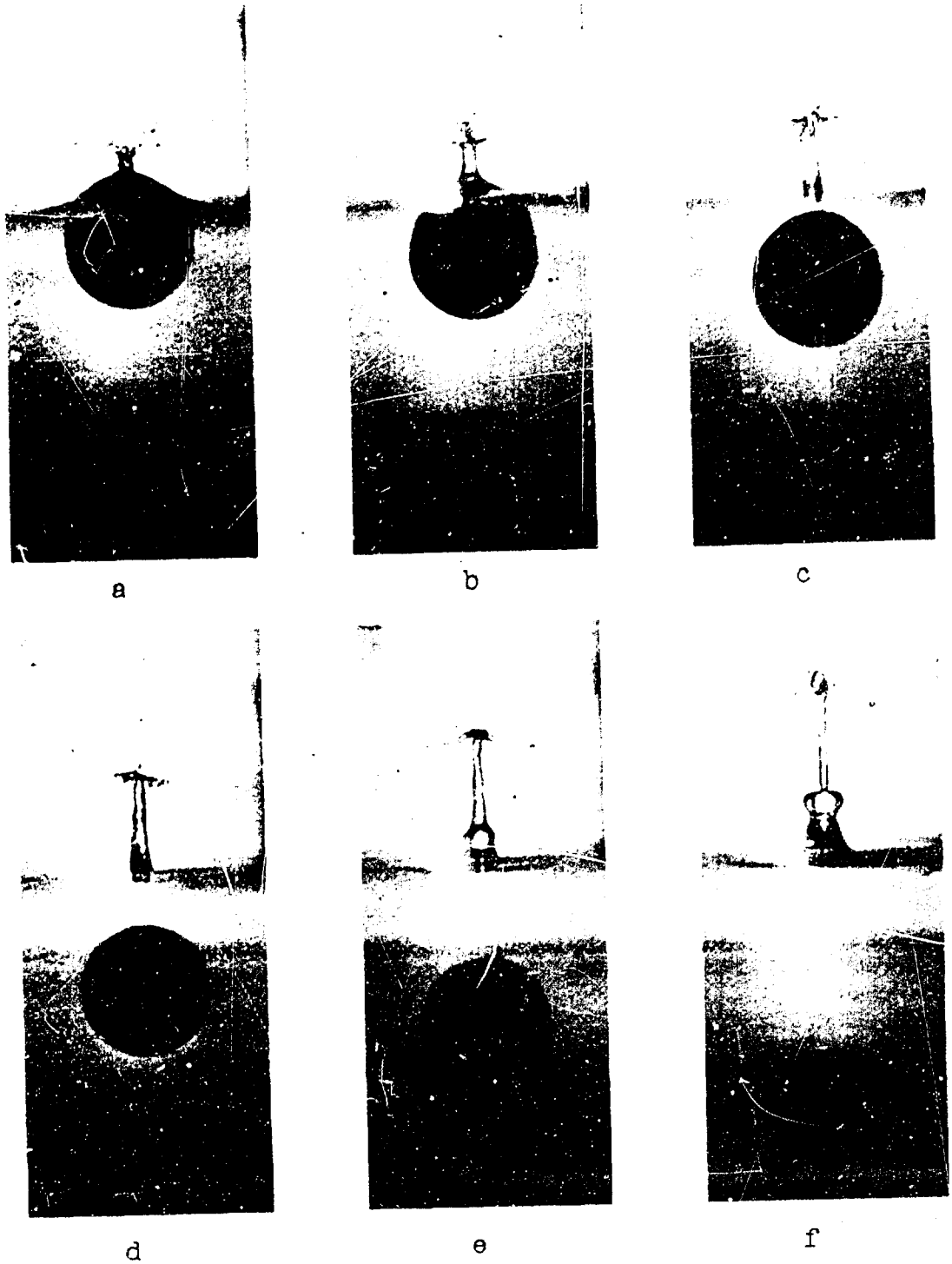

a b c

d e f

SMOOTH ENTRY (Continued)

Steel sphere of diameter 2.86 cm. dropped from a height of 16.2 cm.

Plate 3

MEASUREMENT OF WETTING FACTOR

Depth of penetration = 0.27 radii; Effective depth = 0.35 radii;

Wetting factor = 1.30.

Plate 4

a

b

These pictures were taken by Dr. Furley
of the Morris Dam Group at California Institute of Technology.

Plate 5

ROUGH ENTRY

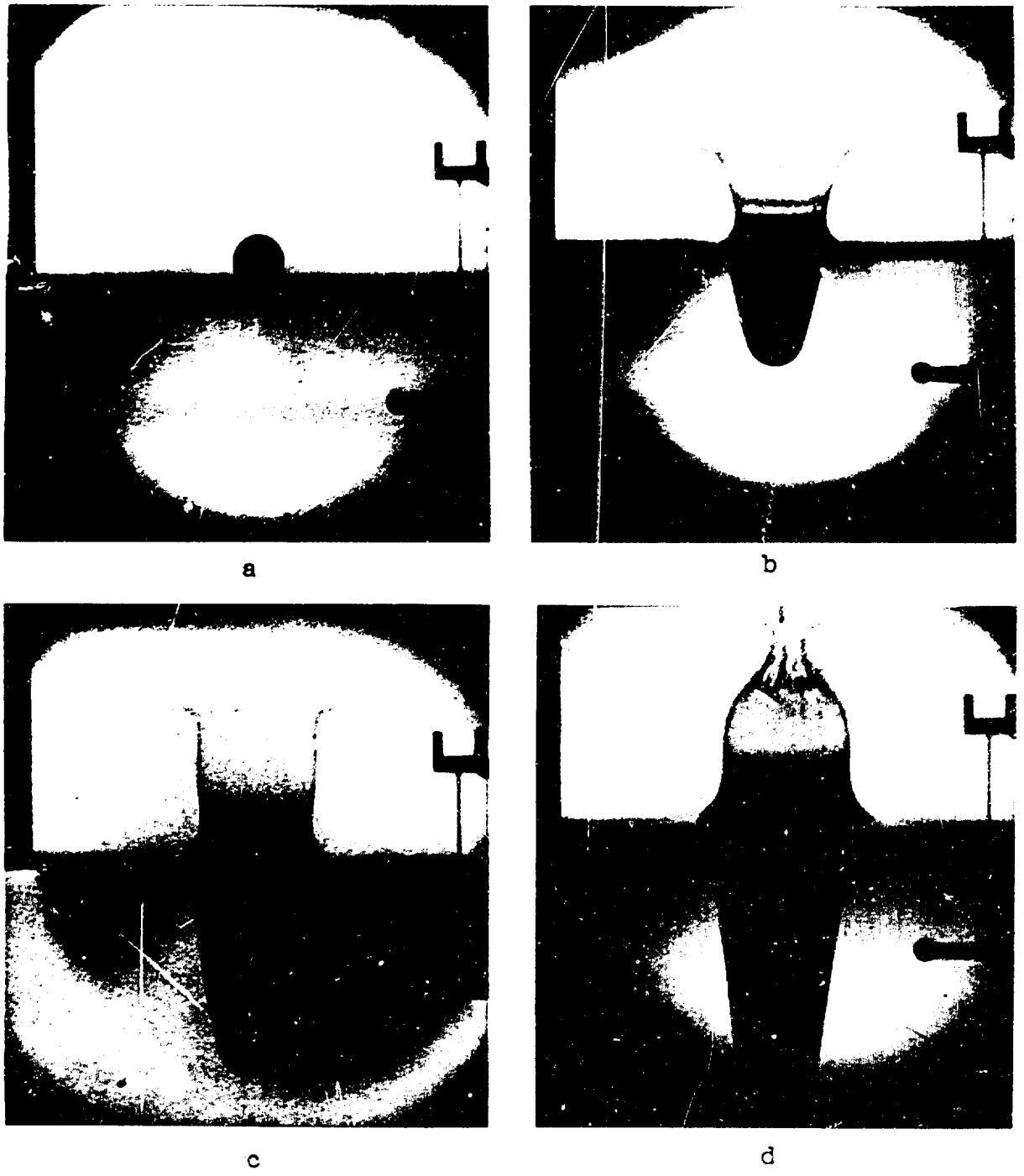

a b c d

Steel ball, 5/8" diameter, velocity 19.4 ft/sec.
Pressure above liquid = 20 cm. mercury.

These pictures were taken by R. M. Davies
of the Engineering Laboratory, Cambridge, England.

Plate 6

HIGH-SPEED ENTRY SHOWING COMPRESSIBILITY EFFECTS

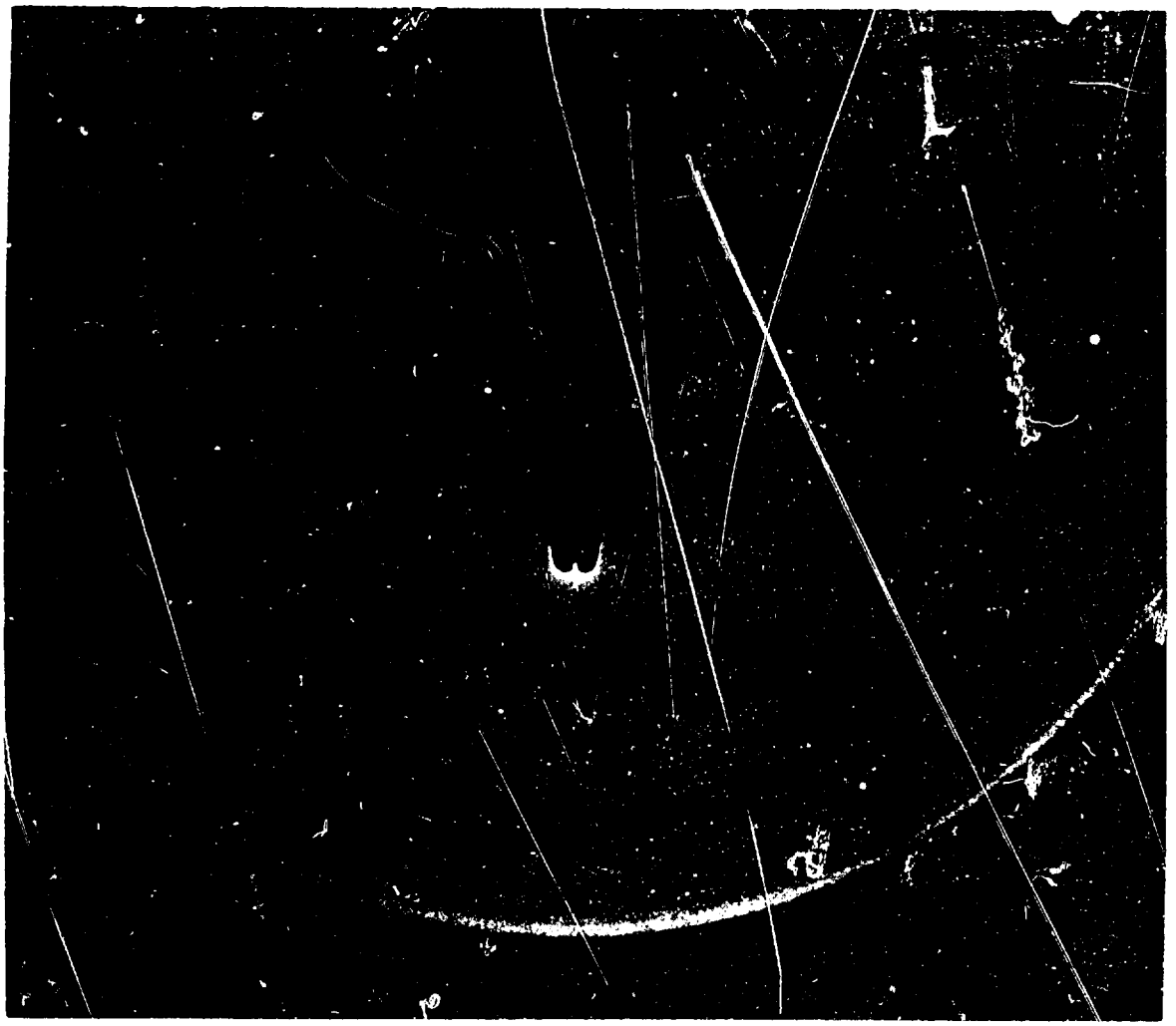

$U_o = 8.84 \times 10^4$ cm/sec. $A = 0.159$ cm. $M_o = 0.6$ grams.

This photograph was taken by E. Newton Harvey
of Princeton University.

Plate 7